

From the hills to the sea: Mineralogical and chemical characterization of a roof tile assemblage from the Byzantine church at Ashdod-Yam (Israel)

Philip Ebeling^{a,*}, Liora Bouzaglou^{b,c}, Dana Ashkenazi^d, Johannes H. Sterba^e, Alexander Fantalkin^c

^a Institute of Classical and Christian Archaeology, University of Münster, Germany

^b Paris 1 Panthéon, Sorbonne, Paris, France

^c Department of Archaeology and Ancient Near Eastern Cultures, Institute of Archaeology, Tel Aviv University, Israel

^d Tel Aviv University, Israel

^e Center for Labelling and Isotope Production, TU Wien, Austria

ARTICLE INFO

Keywords:

Ashdod-Yam
Byzantine church
Ceramic petrography
INAA
Natural pigment
Roof tiles
SEM-EDS

ABSTRACT

This paper presents the results of a multidisciplinary approach characterizing roof tiles excavated at the Ashdod-Yam Byzantine church (Israel). Occupied from the late fourth/early fifth century CE, the building was destroyed by fire toward the end of the sixth century CE, sealed by tiles from the roof's collapse. The assemblage of 3846 roof tiles was initially classified through macroscopic and typological analysis. Selected samples were further subjected to optical microscopy of petrographic samples for provenance studies and ceramic technological insights, along with instrumental neutron activation analysis (INAA). The findings reveal the artifacts to be imported from the eastern Mediterranean ophiolitic complexes and from the Judean Hills. Additionally, fragments of painted ceramic roof tiles were tested using scanning electron microscopy with energy dispersive spectroscopy (SEM-EDS) to assess the composition of the pigments, examine their microstructures, and understand the manufacturing technologies used. Despite the presence of different types of roof tiles, the paint applied to some of them was found to be uniform, consisting of red, ocher-based pigment, likely sourced locally and applied during the roof's construction. This comprehensive examination on a relatively unexplored type of material sheds new light on specific construction choices during the Byzantine period in the southern Levant.

1. Introduction

The archaeological site of Ashdod-Yam (Azotos Paralios/Ashdod by the Sea) is located on the southern coast of Israel (Fig. 1). It is currently surrounded by modern buildings in the southern part of the city of Ashdod and enjoys the status of a protected zone. In the site's southern part there is an artificial mound (acropolis) surrounded by a massive fortification system in the form of a crescent-shaped enclosure, used during the Iron Age IIB–IIC (eighth–seventh centuries BCE) (Fantalkin, 2014, 2018; Fantalkin et al., 2024a; Kaplan, 1969). The Hellenistic period marked another important phase for the site when its acropolis served as a military base during the second century BCE (Ashkenazi and Fantalkin, 2019; Fantalkin et al., 2016, 2024b). The remains of the Roman/Byzantine city, covered by dunes, are spread to the north of the enclosure. During Late Antiquity, which represents the peak of ancient settlement activity at Ashdod-Yam (Bäbler and Fantalkin, 2023), the site

covered at least 2 km from north to south and about 1.5 km from east to west. Ashdod-Yam started as biblical Tel Ashdod's (later known as Azotos Hippenos and Azotos Mesogaios in Greek; Tsafrir et al., 1994:72) harbor but quickly came to exceed its mother city in size and importance during the Roman/Byzantine period. Except for a few burials (Ganor, 2017; Pipano, 1990), until recently archaeological excavations have revealed little about the city during these periods. An impressive citadel (40 × 60 m), which has been identified as the Early Islamic ribat mentioned by al-Muqaddasi (tenth century CE). The citadel was erected over the Byzantine-period remains and excavated by the Israel Antiquities Authority (IAA; Raphael, 2014).

Starting in 2013, a new Ashdod-Yam excavation was launched on behalf of the Institute of Archaeology at Tel Aviv University under the directorship of Alexander Fantalkin.

* Corresponding author.

E-mail address: philip.ebeling@googlemail.com (P. Ebeling).

<https://doi.org/10.1016/j.aia.2024.100040>



Fig. 1. Map of the Ashdod-Yam archaeological site, located on Israel's southern coast (by Liora Bouzagliou).

1.1. The Byzantine church of Ashdod-Yam

In August 2017, during the third archaeological season at the acropolis, it was decided to conduct a limited excavation in the site's northern part, about 1 km northeast of the acropolis and some 350–400 m inland eastward from the coastal line. The excavated area, labeled Area L, was located between modern Ashdod's villas, exactly where >40 years ago traces of mosaic floors were detected during modern construction activities, which damaged the structure's southwestern part. This pilot excavation (permit G-78/2017) yielded evidence for the presence of a Byzantine church, including an almost fully preserved dedicatory inscription in Greek and parts of an additional inscription. Systematic large-scale excavations of the complex undertaken in July–August 2019 and July 2021 (permits G-50/2019 and G-26/2021) focused on the exposure of the entire church complex and related structures.^a As a result, the remains of a large three-aisled basilica-style church with decorative mosaic floors were found, together with an elaborate chapel and additional structures (Fig. 2).

The mosaic floor yielded many dated inscriptions. These provided chronological anchors to the edifice's architectural phases and to events that punctuated its life over almost two centuries (Di Segni et al., 2022). The church measures about 25 × 19 m and is oriented along a general east–west axis. The basilica is divided by two rows of pillars into a wide nave, leading to a *presbyterium/bema* with an apse, flanked by two aisles. A chapel with an apse and two related service rooms, all covered with

mosaic floors, were added to the northern aisle. A wide narthex in the west takes up the complex's full width, including an additional room in the annex's north with a mosaic floor. Together with an estimation of the section destroyed during unsupervised modern construction activity in the 1980s, the total church area reaches about 570 m². Twelve Greek inscriptions were uncovered, with some providing precise dates. A large number of tombs, some containing several deceased individuals, were unearthed at various locations under the church's mosaic floor. Based on epigraphy and numismatic evidence, the building's life span can be estimated as beginning in the late fourth/early fifth century CE and lasting until toward the late sixth century CE. All uncovered parts of the complex showed clear signs of destruction by fire, sealed by the collapse of a large quantity of shattered roof tiles (RTs; Fig. 3). (For more on the roof, see Lorenzon et al., forthcoming.)

1.2. The roof tiles

The majority of the *tegula* and *imbrex* fragments belonged to one of two types of roof tiles, distinguishable by their shape and fabric. Type 1 was of tapering shape, 43 × 29–33 cm in size, with a transversal ridge at an average distance of 3.5–4 cm to the upper end (Fig. 4). This *tegula* type's top surface is slightly smoothed yet has many pores and a sandy matrix. The *imbrices* of this type were only slightly tapering from the dorsal (upper) to the frontal (lower) end, measuring 35 × 11–11.5 cm. Both *tegulae* and *imbrices* were brown to orange in color (Table 1). Some discovered fragments were of different colors, such as yellow and green, caused by overheating during the destruction. Type 1 tiles were predominantly but not exclusively found in the annexes to the northern nave of the church.

The other dominant roof tile type, Type 2, was tapering (39 × 34–38 cm), without a transversal ridge. Its surface was smooth without visible pores (Fig. 5). A handful of fragments of type 2 preserved small stamps on their lower thirds, in a design consisting of circlets, comprised of two close-set semicircles. This type of stamped *tegula* belongs to the larger

^a The Area L excavations within the Ashdod-Yam Archaeological Project framework were directed by Alexander Fantalkin on behalf of the Institute of Archaeology of Tel Aviv University (TAU). The main excavation staff consisted of Liora Bouzagliou (area supervisor, TAU), Yuval Hai and Eli Itkin (field archaeologists, TAU), and Shai Zer (administrator). The inscriptions were translated and interpreted by Dr. Leah Di Segni, and the study of the mosaics was conducted by Dr. Lihi Habas (both of the Hebrew University of Jerusalem).

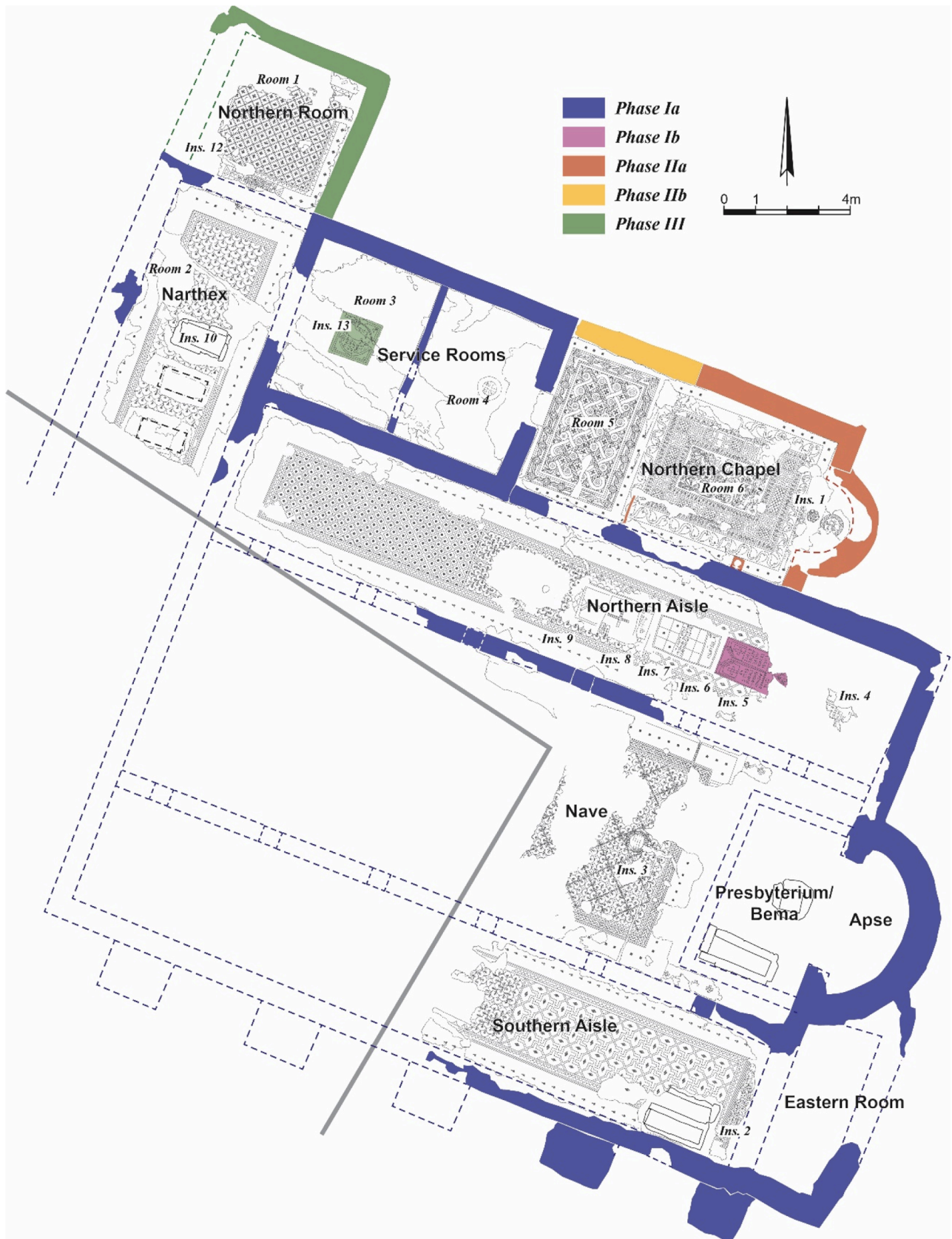


Fig. 2. Plan of the church of Ashdod-Yam, with the locations of inscriptions (by Slava Pirsky and Sergej Alon).

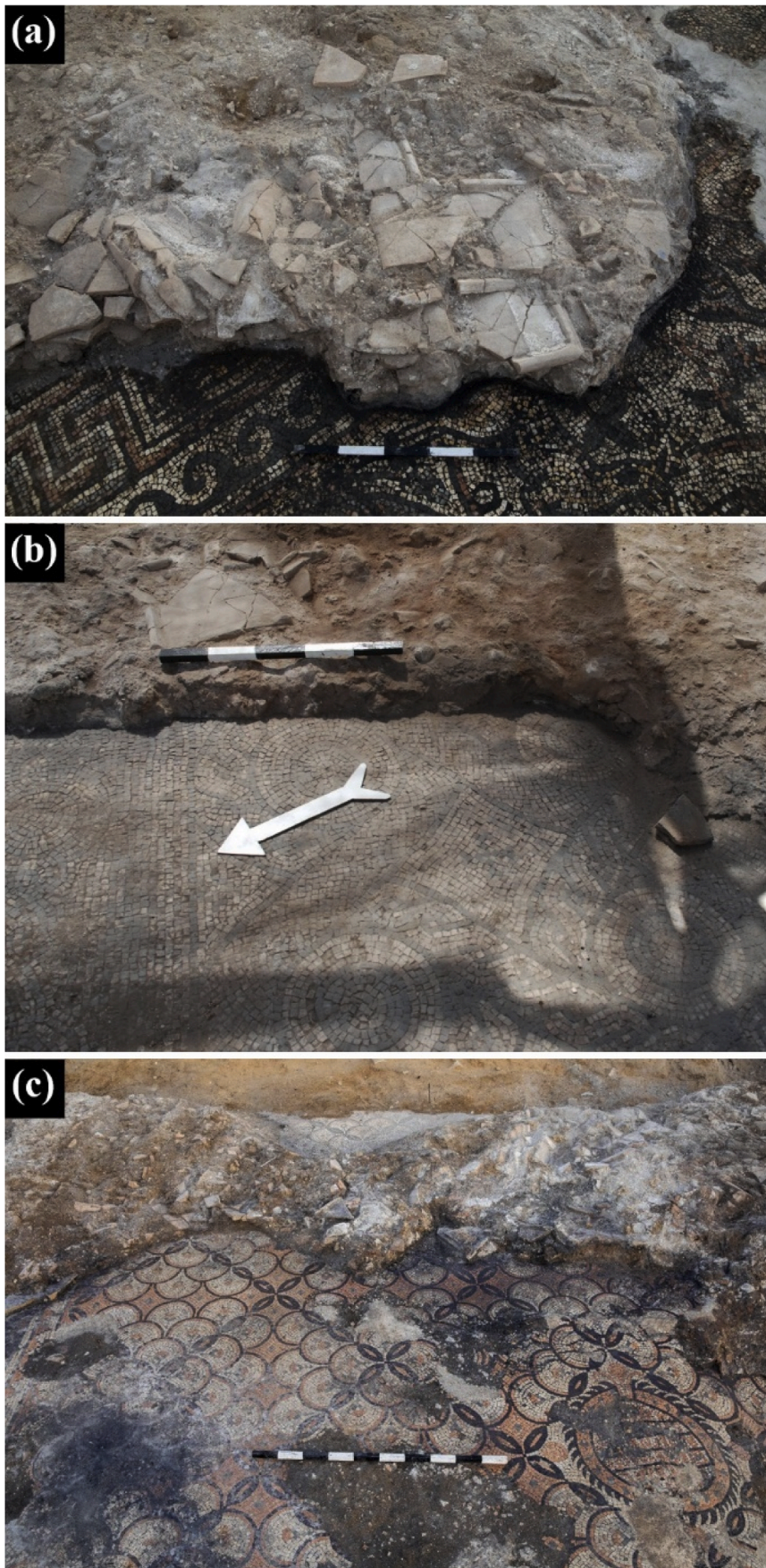


Fig. 3. Traces of mosaic floors discovered in Ashdod-Yam during the excavations: (a) collapsed roof tiles discovered in the northern chapel; (b) collapsed roof tiles discovered at the entrance to the northern chapel; (c) collapsed roof tiles discovered in the nave (photos by Sacha Flit).



Fig. 4. Type 1 roof tiles: (a) preserved example of a *tegula*; red pigments are visible at the right side, above the line of white mortar; (b) a well-preserved *imbrex* (photos by Sacha Flit).

series of geometrically stamped roof tiles and is well-known from other southern Levant sites (Aharoni, 1962:Figure 2.1; Bagatti, 1947:Photo 67.13–18; Clermont-Ganneau, 1899:323, no 3; Fitzgerald, 1931:6; Geva, 2003:Plate 20.1.9; Lombardi, 1957:Fig. 7; Magen, 2015:Plates 60.1–3, 61.1–3; Magen and Baruch, 2012:Plate 2.20; Magen et al., 2012:Figure 53; Mazar, 2007:Figures 7.14.1, 7.31.1, 3–4; 2003:Photo 2.6, Plates 1.1.3–4, 1.5.5–6, 2.3.1; Pele, 2003:Plate 1.20.6–8; Reich and Shukron, 2006:Figures 19.3, 189.1; Saller, 1957:Plate 130.a 4; Saller, 1946: Plate 36.8, 12, 16, 14, 19–20, 22; Tsafir et al., 1979:Figure 27; Vriezen, 1994: Figure 10.1.15–16; Zelinger and Barbé, 2017:Figures 24, 26). Type 2 *tegulae* from the basilica are mostly light beige to red ochre in color, with some appearing bright red. The fabric's beige color, however, was found to be the result of intense heating by fire during the destruction event. Although not many cover tile fragments of this latter type were preserved, comparisons with tiles from other sites (see above) suggest measurements of about 42 × 11–15.5 cm. Type 2 tiles were mostly found within the main nave of the church and were represented by only a few

Table 1

Roof tile groups and macroscopic classification based on optical observation of assemblage from Ashdod-Yam church.

Group	Macro-fabric	Type	Description	Color and Other Traits	Quantification	
Group 1	LOW	<i>tegulae</i>	slightly tapering shape with transversal ridge between the two lateral flanges	brown-orange, heavy weight, hard but sandy fabric	2213 RT	
		<i>imbrices</i>	semicircular/half-tubular		509 RT	
Group 2	YCW/RCW	<i>tegulae</i>	pan tiles	strongly tapering shape	buff-yellow to buff-reddish; very hard fired	961 RT
		<i>imbrices</i>	semicircular/half-tubular		64 RT	
Group 3	YLW/RLW	<i>tegulae</i>	rectangular with transversal ridge between the two lateral flanges	yellow, light weight, soft fabric	89 RT	
		<i>imbrices</i>	gabled/buckled lengthwise		7 RT	
Others	diverse but all micaceous	<i>tegulae</i>	diverse	diverse	5 RT	



Fig. 5. A well-preserved example of a Type 2 *tegula* (photo by Sacha Flit).

fragments within the annexes.

A small number of other *tegulae* types were also found, most notably another ridged type (Type 3; Fig. 6). It is easily distinguishable from the Type 1 pan tiles by the ridge being 5.5–6 cm below the upper rim; thus it is much lower. Also, its bright yellow color, light weight, and soft fabric are distinctive from the brown color, heavy weight, and hard but sandy fabric of Type 1 roof tiles. No *tegula* or *imbrex* of this group was complete

enough to give further evidence about its original morphology.

1.3. Painted roof tiles

Out of the total 3846 collected roof tile fragments, 291 preserved red paint. The red color was preserved on Type 1 fragments much better and more often than on fragments of other types: only 21 fragments of Type 2 and 5 more, out of all the other types, preserved red paint, in comparison with the 265 Type 1 fragments. Additionally, no other type except Type 1 *imbrex* fragments preserved red paint, probably due to its porous fabric properties more than anything else. Twelve such *imbrex* fragments and 253 *tegula* of Type 1, form the majority of objects with preserved pigments. Red color was preserved almost exclusively on top surfaces, including flanges and ridges.

The red paint appeared mostly as straight running lines (148 pieces), not broader than 3 mm. Where observable, most lines were about 11.5–13.5 cm below and parallel to the upper end, running transversally from flange to flange, and on some examples also including the flange exterior surfaces. Similar to these thin lines were broad bands (1–2 cm in width) on 49 fragments. Numerous other fragments (49) preserved the remains of color, suggestive of an entire surface area being covered in red paint, from flange to flange and from the upper end to 11.5–13.5 cm below it. In many of the above examples, the preserved paint was once covered by mortar, which held a *tegula* in place from above and thus preserved the pigments. A few other fragments preserved red lines and areas even in spots on the *tegula* once open to the air and weather, not protected or covered by mortar and other roof tiles. Only seven fragments preserved two crossing lines in the center of the *tegula*. Five more fragments preserved seemingly random marks, maybe letters (*dipinti*) or abstract symbols; none preserved well enough to enable a more precise identification. A single fragment preserved the remains of an inscription, probably in two rows and framed; a single lambda is identifiable; the rest of the letters are illegible. Another six fragments preserved color on their bottom surfaces. The remaining fragments preserved color in unidentified or disintegrated forms of spots and droplets.

The vastly different use of color appears inconclusive and even contradictory. For example, colored areas and remains of color on bottom surfaces suggest that the entire roof tile was covered in red paint, whereas crosses and inscriptions, as well as potential *dipinti* and clear red lines, suggest a more specific use of color and exclude the interpretation of an entirely painted roof tile. Black paint is visible on only seven

fragments, and it appears as covered areas or spots. Nine more fragments may demonstrate black paint or soot. On no fragment does black paint appear alone—red paint is also visible on all 16 of these fragments.

2. Research background

2.1. Previous mediterranean CBM provenance analysis

Ceramic building material (CBM) is a class of fired clay items used for architectural and/or structural purposes and comprising many categories, such as roof tiles, bricks, walls, flue tiles, and water pipes. Although CBM is often encountered in large quantities in field survey and excavation of Classical and Late Antique sites, leading many scholars (often correctly) to assume local production, analyses of plain roof tiles retrieved in the eastern Mediterranean have yet to fully test this assumption. Additionally, most of these rare studies are mono-rather than multi-analytical (see below), unlike the present study, which aims to assess the exact provenance of CBM through optical mineralogy and INAA.

In the southern Levant, only sporadic analyses have been done, starting first in the 1980s on a single roof tile at Tel Keisan (Glass, 1980). Mills conducted a large study aiming to analyze the trade in roof tiles by establishing provenance through clay pastes and thus identifying fabrics from Cilicia, northern Syria, and Cyprus (Mills, 2015a, 2015b). In the same way, an analysis by A. Shapiro of Roman clay sarcophagi and roof tiles from northwestern Galilee and Cyprus revealed production in southern Cyprus or Asia Minor (Shapiro, 1997). Similarly, roof tiles from the synagogues of Horvat Kur (Bes and Braekmans, forthcoming) and Horvat Qana (Edwards, 2009:225–27) were, at least partially, imported products from Asia Minor, probably Cilicia. Northeastern Mediterranean roof tiles were also more recently identified in Group 4 of the assemblage of the Roman-period bathhouse excavated in Khirbet Khaur el-Bak, close to Ashqelon, and the basilica of ancient Ashqelon itself (Cohen-Weinberger et al., 2024). Other imports were from the Beirut region (Group 3), next to two distinct groups of local production (Groups 1 and 2). The thin sections of a few roof tiles from Roman and Byzantine Caesarea were analyzed petrographically by Ben-Shlomo (2006:413–18) and were found to be eastern Mediterranean imports. Due to the lack of petrographic parallels, a more precise location of their provenance was not determined. Petrological studies of the domestic assemblage and roof tiles from a sixth century CE shipwreck at the coast of Dor indicate a Cypriot provenance for the ship, which was presumably returning empty amphorae to Palestine for recycling (Kingsley, 2003; Williams, 2002). Earlier, analysis on a few pieces of CBM from another Byzantine shipwreck off the coast of Tel Dor suggested an Egyptian origin (Barkan et al., 2013:133–34). Recent petrographic and technological analyses of CBM and specialized coarse ware from Caesarea Maritima during the Roman and Byzantine periods revealed a roof tile assemblage made up exclusively of imports from the northeastern Mediterranean (Cyprus, Pisidia, Cilicia, or northern Syria) alongside a minor local production of flue tiles (Bouzaglou, forthcoming). One example from Jordan, from the Early Byzantine tiles from Umm Qeis/Gadara, showed mostly local and interregional CBM (Vriezen, 1995; Vriezen and Mulder, 1997). More recently, the work of Ebeling and Barfod (2022:171–90) on CBM from Jerash in Jordan also revealed mostly local and interregional CBM, just like the Nabataean, Roman, and Byzantine CBM at al-Ḥumayma and Wādī Ramm (Reeves and Harvey, 2016). Holmqvist-Sipilä (2019) conducted energy-dispersive X-ray fluorescence spectroscopy (ED-XRF) and SEM-EDS on a diverse set of pottery objects from the Negev and southern Jordan, including five *tegulae*. They were sampled from objects found at Jebel Harun and Khirbat edh-Dharih. They were all manufactured locally at Khirbat edh-Dharih except for one roof tile, found at Jebel Harun, which belonged to a mineralogical group sampled at Aqaba. The most recent analytical study on CBM and vessels was conducted on a diverse assemblage of objects from the Nabataean to Early Islamic-period site of Khirbet Edh-Dharih in Jordan. It demonstrated that all tested



Fig. 6. Roof tile of Group 3 (photo by Sacha Flit).

objects, from roof tiles to cooking pots, were of local origin and that their clay recipe did not change throughout the centuries (Al-Shorman et al., 2023).

Local roof tile production in the southern Levant, and especially in Jerusalem, has been documented at length (Arubas and Goldfus, 1995, 2005; Seligman, 2015; Tepper et al., 2016). The discovery of a CMB production center at the Jerusalem International Convention Center (Binyanē Ha-Umma) allowed various petrographic studies that shed light on the use of raw material from the Moza formation (Cohen-Weinberger et al., 2020; Goren, 1996a, 1996b). This specific production was identified as belonging to legionary workshops dating to the first and second centuries CE, supplying roof tiles for various Jerusalem-region Roman building activities. A legionary production facility for Legio VI Ferrata and Legio II “Traiana” was similarly documented at Kfar ‘Othnay by Shapiro (2017). In parallel with legionary production, private Jerusalem-area CBM workshops were also operating in the third century CE (Cohen-Weinberger et al., 2022).

2.2. Previous mediterranean roof tile pigment analyses

Although ancient monuments, sculptures, reliefs, and roofs are often reconstructed as painted and covered by vivid colors, evidence of preserved pigments is rare due to persistent attack by urban pollutants and natural degradation processes over time (Ion et al., 2022). Scientific methods are often required to identify pigments related to colors on ancient surfaces. Evidence from the Archaic- through Roman-period central Mediterranean (Italy, Greece, and Turkey) is better published in comparison to areas outside the centers of Greek and Roman culture. However, the colorful roofs of Archaic- and Classical-period temples in ancient Greece cannot be used for a comparison to later CBM since they were colored by clayslip/engobe or wash. A clayslip/engobe is a substance rich in iron oxides, low in calcium oxides, and highly levigated that was applied to pottery vessels and roof tiles. When fired in a kiln it becomes a thin surface layer that seals the surface entirely. A wash is a thin layer of clay, diluted with water up to the point where it becomes a brushable substance. Whereas a wash does not seal surfaces, it is chemically indistinguishable from the clay of the vessel or object it is applied to. Wash is usually not intense in color but remains buff and pale.

The roof tiles from the church of Ashdod-Yam are exceptional in that their painted pigments are indeed preserved; thus comparable evidence is sparse. The closest qualitative parallel comes from a Hellenistic-period shipwreck (Mangalia B) in the Black Sea that carried a set of mostly intact *tegulae* and *imbrices*. The *tegulae* were fully covered in red paint, and probably other substances too, as chemical analyses suggested (Munteanu and Vochițu, 2010). Two other finds are geographically and chronologically closer yet qualitatively not comparable. A single *tegula* fragment from the Byzantine-period monastic complex of Umm Leisun (close to Jerusalem) showed three short strokes of red paint on its surface (Seligman and Gagoshidze, 2015:Fig. 19.2). Two Late Roman to Byzantine-period fragments from a chronologically mixed context of refuse in Jerash/Jordan had red and black paint, suggesting a painted motif (Ebeling and Barford, 2022:185–89). The paint on one of the latter fragments was tested by portable XRF (pXRF) and found to have been based on ochre (red) and ash/coal (black).

3. Analytical methods

The current research aims to characterize the roof tiles retrieved from the Byzantine church at Ashdod-Yam, assessing their mineralogical and chemical composition as well as their microstructure to identify their respective provenance. Additionally, supplementary analyses focused on the mineralogical composition of the pigments used on the roof tiles and the potential reason for their application.

3.1. Provenance studies

To establish the provenance—the place of production—the tested objects’ chemical composition and the identification of inclusions can be used. Arguably, having been made using the same set of raw materials as well as the same recipe and techniques—such as levigation, tempering, and firing temperature—samples similarly produced should result in the same chemical composition and thus originate from the same location, or even the very same workshop. INAA measures the concentrations of up to 30 elements in a sample (the chemical fingerprint; e.g., Mommsen et al., 1995; Perlman and Asaro, 1969; Sterba, 2015). Thin section petrographic analysis (TSPA) enables the scholar to look into the clay and its inclusions, as well as connected evidence. An identification and interpretation of the clay’s contents presents a mineralogical setting that should facilitate identifying its origin location. The following analyses were conducted.

Macroscopic fabric analysis studies the fabric’s petrographic composition at low magnification (ca. x10–50). This method is used to characterize and classify ceramics and reconstruct aspects of their technology (see Quinn, 2022:152–62 for the methodology). The analysis was realized with a hard lens, with a stereomicroscope (Dino-Lite digital microscope model AM4113T, up to 200x magnification, and model AM4113T5, with a fixed 500x magnification) on 17 samples (Table 2), and with the naked eye on 3846 roof tiles. The fabrics were characterized and interpreted macroscopically on fresh breaks by recording their colors, textures (hardness, fracture), the nature of the inclusions (type, relative abundance, modal grain size, shape, and degree of sorting), clay matrix, and voids (Table 1).

Seventeen roof tiles were analyzed using TSPA (see supplementary material). Samples were polished, affixed to a glass slide, and then ground to reach a standard thickness of 30 μm (Quinn, 2022:23–36). The thin sections were then examined under a polarizing light microscope to reveal aspects related to their provenance and manufacturing technology, including their raw materials selection, paste preparation, forming, surface finish, and firing methods (Quinn, 2013:81–93). The classification according to petro-fabrics was realized by describing the characteristics of the matrix (clay background, plastic inclusions) and inclusions such as temper and non-plastic components. (For the methodology, see Goren et al., 2004:9–17; Quinn, 2022.)

Six samples (Tables 2–4) were submitted for INAA. All samples had been taken on-site by drilling with a corundum drill bit. The collected drilling dust was sent to the Center for Labelling and Isotope Production (CLIP) laboratory at the TRIGA Center Atominstitut in Vienna. At CLIP, the samples were analyzed (Table 3) following the regular protocol for archaeological ceramics (Sterba, 2018). Sample irradiation was done for 35 h at a neutron flux density of $1 \cdot 10^{13} \text{ cm}^{-2} \text{ s}^{-1}$ and, after cooling times of four and 40 days, measurements of the samples were performed for 1800 s and 10000 s, respectively. For quantification and comparability with the database, the Bonn Standard reference material (H. Mommsen and Sjöberg, 2007) was used.

3.2. Pigment analysis

In the last few decades, the use of both destructive techniques (DT) and non-destructive techniques (NDT), combined with multidisciplinary approaches (archaeological, material characterization, geological, and petrographic), has provided a more comprehensive interpretation of ceramic materials and pigments (Domingo and Chieli, 2021). In this study, the red pigments on roof tiles were studied and analyzed by both DT and NDT techniques. The analyses are described below.

Visual testing (VT) inspection of the Type 1 and Type 2 roof tile fragments and the painted colors on top (Fig. 7) was carried out to observe the samples’ overall quality and to detect visible characteristics that might assist in understanding various aspects of the objects.

To build a catalog of the ceramic substrates and pigments and to visually compare the pigments to the available literature, the surfaces of

Table 2

Roof tiles analyzed through optical mineralogy, affiliated petro-fabric with provenance, and INAA results.

ID	Reg. No.	Tile Type and Macro-fabric	Petro-fabric	Suggested Provenance	INAA
RT1	66–1428–6	tegula, body; Type 2; YCW/RCW	A1	Judean Hills, (Jerusalem/Hebron regions)	HebA/Edom
RT2	153–2090–15	imbrex, body; Type 2; YCW/RCW	A3	Judean Hills, (Jerusalem/Hebron regions)	single
RT3	172–1987–2	tegula, upper rim; Type 1; LOW	C1	Cilicia, Cyprus, or northern Syria	/
RT4	42–1651–9	tegula, flange; Type 2; YCW/RCW	A1	Judean Hills, (Jerusalem/Hebron regions)	single
RT5	163–1952–20	tegula, upper rim; Type 3; YLW/RLW	B	Cyprus	/
RT6	134–1748–2	imbrex, rim; Type 1; LOW	C2	Cilicia, Cyprus, or northern Syria	/
RT7	66–1591–23	imbrex, rim; Type 1; LOW	C2	Cilicia, Cyprus, or northern Syria	single
RT8	131–1622–6	imbrex, rim; Type 2; YCW/RCW	A3	Judean Hills, (Jerusalem/Hebron regions)	/
RT9	126–1578–1	tegula, flange; Type 2; YCW/RCW	A2	Judean Hills, (Jerusalem/Hebron regions)	/
RT10	66–1591–37	tegula, body; Type 2; YCW/RCW	A1	Judean Hills, (Jerusalem/Hebron regions)	/
RT11	110–1634–1	tegula, body; Type 1; LOW	C3	Cilicia, Cyprus, or northern Syria	single
RT12	108–1542–2	tegula, upper rim; Type 1; LOW	C2	Cilicia, Cyprus, or northern Syria	/
RT13	131–1622–5	tegula, body; Type 2; YCW/RCW	A1	Judean Hills, (Jerusalem/Hebron regions)	/
RT14	110–1634–2	tegula, body; type 3; YLW/RLW	B	Cyprus	single
RT15	117–1517–2	tegula, flange-rim corner; Type 2; YCW/RCW	A1	Judean Hills, (Jerusalem/Hebron regions)	/
RT16	110–1497–23	tegula, flange; Type 1; LOW	C4	Cilicia, Cyprus, or northern Syria	/
RT17	130–1616–5	tegula, flange; other type	D	Egypt	/

Note: YCW/RCW, LOW, and YLW/RLW represent macroscopically observed ware groups based on color and other properties of the fired roof tiles.

the fragments were photographed in daylight using a Canon 6D camera with an EF 40 mm 1/2.8 STM lens and XIT extension macro ring (65 mm) equipment. Additionally, stereomicroscope observation of the samples was executed with a Discovery V8 Zeiss instrument with a total zoom magnification range of $\times 6.3$ to $\times 50.4$. Each sample's transverse cross section (T-CS) and planer section (P-section) were observed.

SEM observation with EDS chemical analysis was performed with an environmental SEM (ESEM). The examination was carried out in low-vacuum mode. The roof tile fragments were characterized by an FEI Quanta 200FEG ESEM instrument equipped with an Everhart–Thornley secondary electron (SE) detector, during which both SE and back-scattered electron (BSE) modes were applied. The EDS examination was done with an Si (Li) liquid-cooled Oxford X-ray detector.

4. Results

4.1. Macroscopic classification and characterization

Primary macroscopic classification of 3846 roof tiles from the church allowed the determination of three main macro-fabrics (Fig. 8, Table 1).

Group 1, classified as Light Orange Ware (LOW), is the most abundant, comprising 2213 *tegulae* and 509 *imbrices*. These tiles are characterized by a brown-orange coloration, a hefty weight, and a sandy yet hard fabric, with the *tegulae* exhibiting a slightly tapering shape and a transversal ridge between two lateral flanges (Figs. 4, 8:RT3, 6, 7, 11, and 12). Group 2, designated as Yellow/Red Clean Ware (YCW/RCW), includes 961 *tegulae* and 64 *imbrices*. These tiles show a buff-yellow to buff-reddish hue and are distinctive for their substantial tapering form and hard firing (Figs. 5, 8:RT1, 4, 8, 9, 10, and 13). Group 3, termed Yellow/Red Light Ware (YLW/RLW), is considerably less represented, with 89 *tegulae* and seven *imbrices*, distinguished by a yellow color, a light weight, and softer fabric (Figs. 6, 8:RT5, and 14). The *tegulae* in this group are rectangular with a transversal ridge between the lateral flanges, while the *imbrices* are buckled lengthwise. The “others” category encompasses a small assemblage of five *tegulae* of varying appearances, all of which presented a micaceous composition.

4.2. TSPA

Following the macroscopic classification and characterization, 17 samples were selected for TSPA from all groups (Table 1, Groups 1–3 and “others”). Four petrographic groups (petro-fabrics Groups A–D) with subvariants were identified based on their mineralogical composition (Tables 2, 5, and 6 and Fig. 9; see supplementary material). This section is arranged by each petro-group's petrographic characterization and suggested provenance.

4.2.1. Petro-group A

This petro-group is characterized by a clayey matrix and the presence of rhombohedral dolomite crystals (Figs. 8, 9; Table 5). All samples were taken from YCW/RCW/Type 2 roof tiles. It was identified as coming from a marl unit of the Cenomanian Moza formation (Arkin et al., 1965; Arkin and Ecker, 2014; Ben-Shlomo and Mommsen, 2018:356 [Group 2b]; Ben-Shlomo et al., 2022 [Group 5]; Ben-Tor, 1945, 1966; Cohen-Weinberger et al., 2017:9–10 [Group A]; 2020, Groups A–B; Cohen-Weinberger and Rosenthal-Heginbottom, 2019; Goren, 1995; Goren et al., 2004:262–64). The fabric's main feature is the rhombohedral dolomite crystals, appearing in various quantities from rare to abundant. They are common in the overlying Aminadav formation as well as in other Cenomanian units of the Judean Hills (Ben-Tor, 1945). The dolomitic sand's state of preservation indicates that it developed in situ, without translocation processes (Ben-Tor, 1945). Nevertheless, its alteration into calcite in most cases indicates either a high firing temperature (above 750–800 °C) during manufacture or a refiring during the church's destruction. Within the Cenomanian Judea group, the Aminadav formation (upper) is stratigraphically located above the Moza clay and marl and the lower Beit Meir dolomite. This sequence supports their mixing, as already identified in the pottery industry (Ben-Tor, 1966:48–52; Cohen-Weinberger et al., 2020). Also, the argillaceous nodules of *terra rossa* occurred in previous petrographic analyses of vessels made of Moza clay (Cohen-Weinberger et al., 2020; Goren, 1996a:51, 1996b:149).

A comparison with previously examined roof tiles from the Jerusalem Convention Center excavations (Cohen-Weinberger et al., 2017 [Group A]; 2020 [Groups A and B]) reveals a high degree of lithological similarity between these samples and the roof tiles discussed here. The use of Moza clay (Cohen-Weinberger et al., 2020 [Subgroups A1–A3]) was common during the Hasmonean and Early Roman periods (Strata VIII–VI) and is generally assigned to a Judean Hills provenance. Hence, samples belonging to this category were considered regionally imported

Table 3
Elemental chemical composition of the six samples measured by INAA.

	2023/14_VAR/AYS/ 011B 66-1428-6	2023/14_VAR/AYS/ 012B 153-2090-15	2023/14_VAR/AYS/ 013B 42-1651-9	2023/14_VAR/AYS/ 014B 66-1591-23	2023/14_VAR/AYS/ 015B 110-1634-1	2023/14_VAR/AYS/ 016B 110-1634-2
As	7.06 ± 0.465	12.4 ± 0.819	11.1 ± 0.73	11.3 ± 0.747	11.2 ± 0.739	14.5 ± 0.955
Ba	386 ± 7.26	602 ± 11.3	492 ± 9.23	305 ± 5.73	314 ± 5.89	638 ± 12
Ce	45.4 ± 0.547	35.7 ± 0.431	55.6 ± 0.67	40.2 ± 0.485	42.8 ± 0.516	37.1 ± 0.447
Co	12.9 ± 0.103	36.5 ± 0.29	13.8 ± 0.109	60.9 ± 0.483	47.7 ± 0.378	19.7 ± 0.156
Cr	83.2 ± 2.92	1120 ± 39.3	94.4 ± 3.31	3760 ± 132	2840 ± 99.8	290 ± 10.2
Cs	3.47 ± 0.0374	3.45 ± 0.0372	2.06 ± 0.0222	1.95 ± 0.021	2.61 ± 0.0281	1.2 ± 0.013
Eu	1.06 ± 0.013	0.828 ± 0.011	1.29 ± 0.016	0.568 ± 0.0072	0.731 ± 0.0092	0.975 ± 0.0123
Fe	33,200 ± 529	52,200 ± 832	37,800 ± 603	55,100 ± 879	51,000 ± 814	41,500 ± 662
Hf	5.33 ± 0.15	2.51 ± 0.0707	5.22 ± 0.147	1.59 ± 0.0448	2.35 ± 0.0661	2.97 ± 0.0838
K	24,600 ± 431	12,600 ± 220	29,000 ± 509	7260 ± 127	9770 ± 171	10,700 ± 187
La	22.1 ± 0.582	17.2 ± 0.452	28.5 ± 0.75	11.6 ± 0.305	15.9 ± 0.418	20.1 ± 0.529
Lu	0.37 ± 0.0161	0.265 ± 0.0115	0.438 ± 0.0191	0.165 ± 0.0072	0.256 ± 0.0112	0.371 ± 0.0161
Na	1570 ± 33.2	6660 ± 140	1220 ± 25.6	4310 ± 90.8	6610 ± 139	6370 ± 134
Nd	18.5 ± 0.66	12.4 ± 0.445	19 ± 0.677	11.4 ± 0.41	21.7 ± 0.777	16.1 ± 0.574
Ni	40.4 ± 0.423	493 ± 5.16	35.9 ± 0.376	1120 ± 11.8	802 ± 8.39	192 ± 2.01
Rb	58.6 ± 1.19	47.8 ± 0.968	53.3 ± 1.08	28.7 ± 0.582	41.9 ± 0.849	24.8 ± 0.502
Sb	0.258 ± 0.0146	0.588 ± 0.0333	0.292 ± 0.0165	0.417 ± 0.0236	0.566 ± 0.032	0.832 ± 0.0471
Sc	14.1 ± 0.298	17.5 ± 0.37	16.8 ± 0.356	16.9 ± 0.359	16.8 ± 0.356	17.9 ± 0.379
Sm	3.99 ± 0.142	2.68 ± 0.0953	5.1 ± 0.181	1.91 ± 0.0677	2.62 ± 0.0929	3.58 ± 0.127
Sr	198 ± 10.53	15 ± 16.6	162 ± 8.55	268 ± 14.2	350 ± 18.5	448 ± 23.7
Ta	0.714 ± 0.0137	0.512 ± 0.0098	0.826 ± 0.016	0.348 ± 0.0067	0.471 ± 0.0090	0.553 ± 0.0106
Tb	0.616 ± 0.0114	0.473 ± 0.0087	0.743 ± 0.014	0.308 ± 0.0057	0.453 ± 0.0083	0.552 ± 0.0102
Th	6.2 ± 0.133	5.16 ± 0.111	7.79 ± 0.167	3.27 ± 0.0702	4.56 ± 0.0978	5.6 ± 0.12
Ti	10,600 ± 489	7140 ± 329	9410 ± 434	5410 ± 249	7350 ± 338	10,300 ± 474
U	1.88 ± 0.14	1.12 ± 0.0829	1.74 ± 0.129	0.853 ± 0.0634	1.1 ± 0.0816	2.24 ± 0.167
W	0.892 ± 0.0545	1.06 ± 0.0647	2.16 ± 0.132	0.934 ± 0.057	0.668 ± 0.0408	1.12 ± 0.0684
Yb	2.21 ± 0.0355	1.82 ± 0.0293	2.53 ± 0.0407	1.93 ± 0.031	1.54 ± 0.0247	2.37 ± 0.0382
Zn	60.7 ± 0.844	81.6 ± 1.13	50.4 ± 0.7	77.2 ± 1.07	80.1 ± 1.11	74.1 ± 1.03
Zr	152 ± 6.38	81.9 ± 3.43	156 ± 6.55	50.2 ± 2.1	62.5 ± 2.6 2	105 ± 4.41

Note: All concentrations and measurement error values are presented in µg/g.

Table 4
Description of examined Roof Tiles with Paint on Top Retrieved from the Byzantine Church at Ashdod-Yam and Suggested Provenance of Raw Material Based on Petrographic Results.

Roof Tile ID	Registration No.	Type	Description	Suggested Provenance
Sample 1 (Type 1 RT2)	153-2090-15	<i>imbrex</i> , LOW	covered with red paint	Cilicia, Cyprus, or northern Syria
Sample 2 (Type 1 RT)	153-2090-9	<i>tegula</i> , LOW	covered with red paint	Cilicia, Cyprus, or northern Syria
Sample 3 (Type 2 RT1)	66-1428-6	<i>tegula</i> , YCW/RCW	covered with red and black paint	Judean Hills, Jerusalem/Hebron region
Sample 4 (Type 2 RT)	134-1675-12	<i>imbrex</i> , YCW/RCW	covered with mortar remains and red paint	Judean Hills, Jerusalem/Hebron region
Sample 5 (Type 1 RT)	153-1881-4	<i>tegula</i> , LOW	covered with mortar remains and red paint	Cilicia, Cyprus, or northern Syria
Sample 6 (Type 1 RT)	36-1182-9	<i>tegula</i> , LOW	covered with mortar remains and red paint	Cilicia, Cyprus, or northern Syria
Sample 7 (Type 1 RT)	36-1182-8	<i>tegula</i> , LOW	covered with red paint	Cilicia, Cyprus, or northern Syria

Notes: Imported tiles from the eastern Mediterranean are Type 1/Petro-group C, and tiles from the Judean Hills are Type 2/Petro-group A. LOW and YCW/RCW refer to ceramic tile color.

from the Judean Hills—probably from the Jerusalem region and also plausibly from the Hebron region (see below). The use of this clay type in the region therefore indicates a technical continuity with traditions identified as occurring during the Roman period and in particular with the legionary CBM production in Jerusalem (Cohen-Weinberger et al., 2020).

4.2.2. Petro-group B

This group is characterized by a clayey matrix and the ubiquitous appearance of detrital ophiolites and mudstones, perhaps deliberately added to the pastes for tempering effects (Figs. 9, 10; Table 5). All samples were taken from YLW/Type 3 roof tiles. Mudstones have been well attested as natural inclusions or intentional temper in various eastern Mediterranean ceramics, especially in Cyprus (Jacobs and Borgers, 2015; Makarona et al., 2016; Xenophontos et al., 2000). Generally reported for large to medium-size, thick-walled, hand-formed vessels, the addition of mudstone is a technical means to reduce clay plasticity and avoid cracking during the drying process (Makarona et al., 2016; Whitbread, 1995). In Cyprus, mudstones are primarily found in ceramics attributed to sites within the Mamonia terrane, a distal, off-axis extension of the Troodos complex's main Cretaceous ophiolite outcrop, located in the island's southwest, where mudstone outcrops are abundant. Outcrops of radiolarian mudstones are found in the Agios Fotios and the Diarizos group of the Mamonia terrane, both of the Cretaceous-Triassic age, and in the Xeropotamos and Diarizos river valleys as well. Mudstones were identified in the Troodos ophiolites complex itself, within the Perapedi formation and the Moni mélange (Garzanti et al., 2000:206; Nodarou, 2017). Yet the precise production location cannot be assessed due to the lack of petrographic parallels and the deliberate addition of mudstones to the clay recipe. However, the morphology of 89 *tegulae* and *imbres* fragments of this petro-group is comparable to the "yellow tiles" known from several excavations and studies on Cyprus (Manning et al., 2002:60; Rautman et al., 1993:Figure 3.22; 1999). Their production site was likely located in the eastern Mesaoria plain, not far from Salamis, based on the combination of the reworked ophiolitic and bioclastic material's very weathered nature and the presence of the calcareous, fine-grained, clay-rich Neogene and Pleistocene sediments that crop out in the Mesaoria plain (Rautman et al., 1999). Pliocene and Neogene marls can also be found in the sediments flanking the Kyrenia range in the island's north. They exist south of the Troodos Mountains as well and are also interspersed among the Mamonia Complex rocks in the

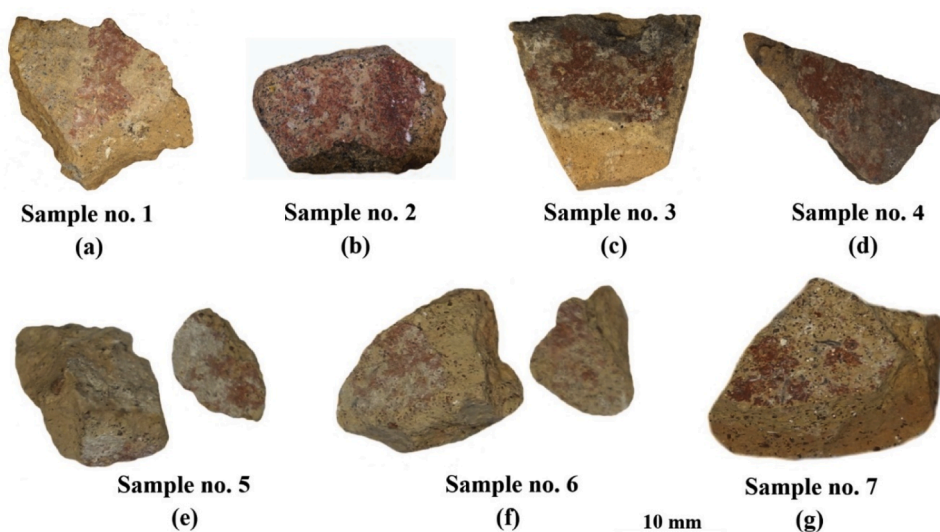


Fig. 7. Byzantine roof tile fragments preserving pigments: (a) Sample 1 (*imbrex*, imported RT Type 1, 153–2090–15), covered with red decoration; (b) Sample 2 (*tegula*, imported RT Type 1, 153–2090–9), covered with red paint; (c) Sample 3 (*tegula*, local/regional RT Type 2, 66–1428–6), covered with red and black paint; (d) Sample 4 (*imbrex*, local/regional RT Type 2, 143–1675–12), covered with red and black paint; (e) Sample 5 (*tegula*, imported RT Type 1, 153–1881–4), covered with red paint; (f) Sample 6 (*tegula*, imported RT Type 1, 36–482–9), covered with red paint; (g) Sample 7 (*tegula*, imported RT Type 1, 36–482–8), covered with red paint (photos by Dana Ashkenazi).

west (Vaughan, 1987). Still, the evidence suggests the region of ancient Salamis in eastern Cyprus as Petro-fabric B's tentative place of origin.

4.2.3. Petro-group C

This petro-group, corresponding to LOW/Type 1 roof tiles, is characterized by a clayey matrix and a sandy fraction dominated by a basic to ultra-basic source, including dominant red-orange serpentine (derived from the alteration of pyroxene and olivine) and iddingsite (from the alteration of olivines), as well as clinopyroxenes (altered in some cases into serpentine). It is also characterized, to a lesser degree, by igneous rock fragments (primarily basic but also rare ultra-basic and intermediate rocks), orthopyroxenes (sometimes altered into serpentine), and amphiboles, sometimes rubefacted with strong pleochroism. The internal variability in this petro-fabric group allows its division into four subgroups (C1–C4; see Fig. 9, Table 5, and supplementary material). Its particular set of inclusions suggests that this petro-fabric derives from ophiolitic rock sequences. Ophiolites are geological formations that consist of rocks formed at or near Earth's oceanic crust and the underlying mantle. Usually found in mountain belts, they are thought to be formed when the oceanic crust and mantle are thrust onto the continental crust during the process of tectonic plate collision (Coleman, 1977; Dilek and Furnes, 2014; Dilek and Eddy, 1992; Miyashiro, 1975; Moores, 1982; Nicolas, 2012; Nicolas and Boudier, 2003). In the eastern Mediterranean, ophiolite sequences are found in Cilicia (the Mersin and Pozanti-Karsanti massifs), Pisidia (the Kizildağ massif in the Amanus range's southwestern part), northwestern Syria (the Baër-Bassit massif, south of the lower Orontes plain), and southwestern Cyprus (Troodos massif; Mikhailov and Ponikarov, 1986; Parrot, 1977; Şenel, 2002; Tekeli and Erendil, 1986; Whitechurch et al., 1984). Similar petro-graphic results were published for Group 4 of Roman-period CBM from Khirbet Khaur el-Bak and the basilica of Ashqelon (Cohen-Weinberger et al., 2024:13, 16–17).

4.2.4. Petro-group D

This petro-fabric is a unicum derived from a micaceous soil, to which a coarsely crushed temper was added (Fig. 9, Table 5, and supplementary material). The mineralogical composition seems to be consistent with Egyptian production, but a more precise production location cannot be assessed yet. This group was produced with the so-called Nile silt (or, preferably, Nile mud). This term refers to pottery manufactured

in Egypt from local Quaternary Nile sediments (Arnold and Bourriau, 1993:148–82; Bourriau et al., 2000). The materials also contain high proportions of ferrous minerals and organic matter that provide dark reddish-brown or even black products under a reducing firing atmosphere. The information about the clay types used for Egyptian ceramics throughout the periods is well established (Arnold and Bourriau, 1993:148–82; Bourriau et al., 2000). Similar base clay, although without the coarse fraction, was used for the production of Byzantine amphorae from Aswan/Elephantine (Peloschek, 2015). A small set of brick-like objects from a Byzantine shipwreck off the coast of Tel Dor, probably used on board for cooking, was tested petrographically and found to be from Egypt (Barkan et al., 2013:133–34). The erosion of the single tested fragment associated with this petro-fabric precludes the development of further information. The sample was taken from the group of 'other' roof tiles.

4.3. INAA, Tables 2 and 3

Results of the INAA are presented in Table 3. The comparison of the samples 2023/14_VAR/AYS/011B to /016B (reg. nos. 66–1428–6, 153–2090–15, 42–1651–9, 66–1591–23, 110–1634–1, 110–1634–2) to the database resulted in only one sample (2023/14_VAR/AYS/011B or 66–1428–6, Sample 3, Type 2, RT1) being correlated to an already established group or provenance (see Table 2). The other five samples have no similar chemical pattern match in the existing database. The group HebA is localized around Tel Hebron by the analysis of wasters (see Ben-Shlomo, 2020; Ben-Shlomo and Mommsen, 2018, 2019; Mommsen and Ben-Shlomo, 2020).

4.4. Pigment analysis: VT and color catalog

VT of the roof tile fragments (Fig. 7) revealed differences between the ceramic material of Type 1, made from the eastern Mediterranean ophiolitic regions, and that of Type 2, made from the Judean Hills substrate. Type 1 roof tile fragments are made of clay with a coarse surface that includes many voids and large pores reaching up to 1 mm in diameter (Fig. 10c, Fig. 10i). The roof tile fragments of Type 2 are made of fine and homogeneous material and are less porous than those of Type 1 (Fig. 10d). However, VT observation of the red-painted areas revealed the use of similar colors on both roof tile types, with a tone typical of red

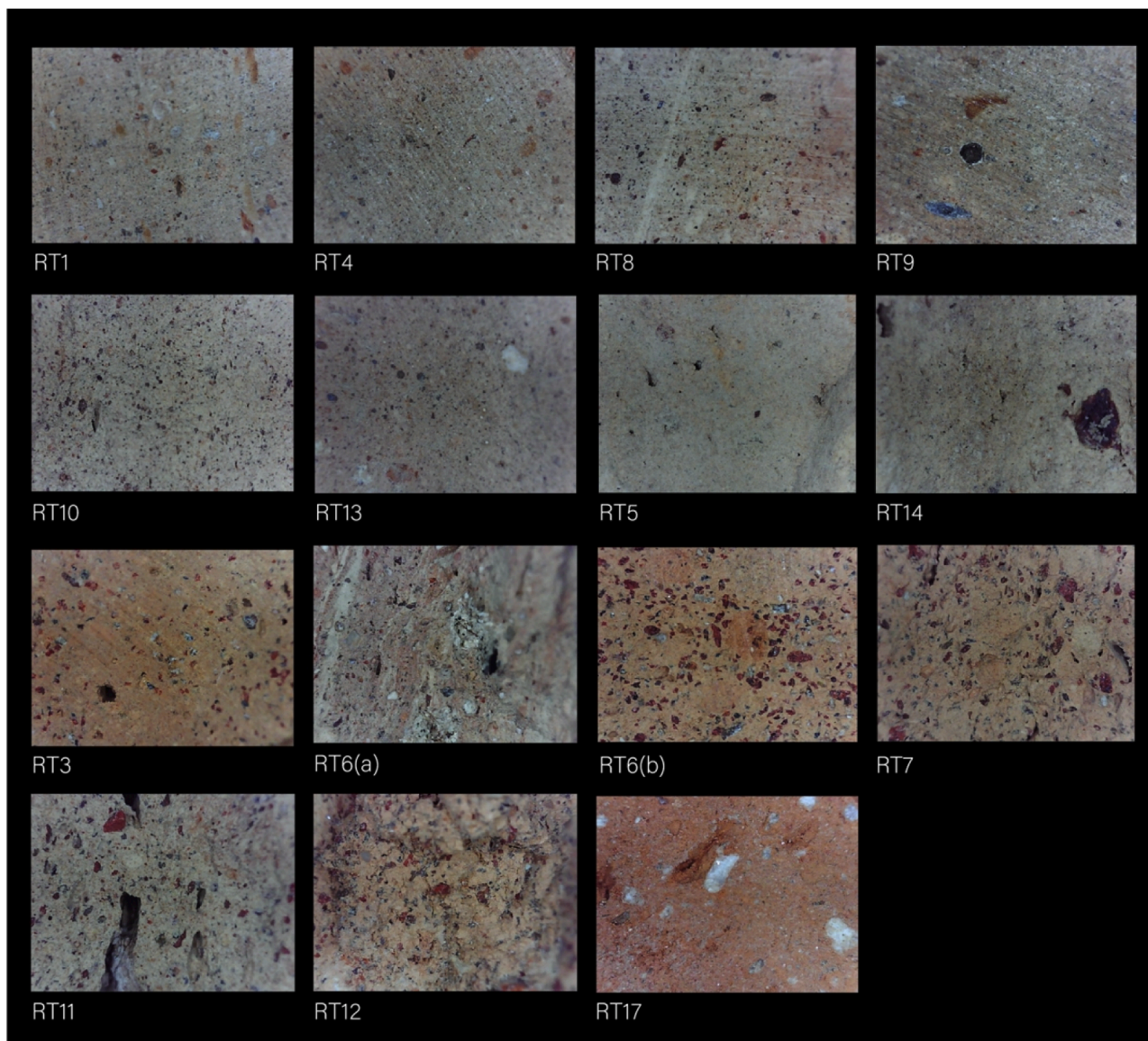


Fig. 8. Stereomicroscope pictures of macro-fabrics (Group 2: RT1, 4, 8, 9, 10, and 13; Group 3: RT5 and 14; Group 1: RT3, 6, 7, 11, and 12; outlier: RT17) (photos by Liora Bouzaglou).

ocher pigment (Ashkenazi et al., 2021; Giumlia-Mair et al., 2022:112).

The close-up photos of the roof tiles (Figs. 9 and 10) and their stereomicroscope observation (Fig. 11) show lots of inclusions as well as red and black paint covers on their surfaces. Remains of white mortar were also observed on the surface of both types; see Sample 2 (Fig. 10c), Sample 3 (Fig. 10e), Sample 5 (Figs. 10g and 11d), Sample 6 (Figs. 10h and 11e), and Sample 7 (Figs. 10i and 11f). Although there were differences between the Type 1 and Type 2 ceramic materials, they shared similar pigment colors and texture (Figs. 10 and 11).

4.5. SEM-EDS analysis (Table 6)

The SEM observation of the red paint (Figs. 12–16) was conducted on all samples, and it was found to be red pigment (Table 6). The pigment particles ranged in size from 0.2 to 1 μm (small) to 1–10 μm (large). An area of black paint was observed on Sample 4 (Type 2; Figs. 10f, 15c–d; BSE mode) and found to be carbon black.

The analysis of Type 1 tile red paint revealed a composition of 27.8–71.4 wt% Fe_2O_3 , 4.3–9.6 wt% Al_2O_3 , 10.5–24.9 wt% SiO_2 , and 9.4–26.9 wt% CaO , and some K_2O , MgO , MnO (Table 6). The analysis of

Type 2 tile red paint revealed a composition of 11.2–46.0 wt% Fe_2O_3 , 7.7–12.5 wt% Al_2O_3 , 16.5–20.6 wt% SiO_2 , 17.5–52.3 wt% CaO , and TiO_2 , K_2O , and MgO . The SEM-EDS analysis results of the black paint concluded with a composition of 4.8 wt% Al_2O_3 , 10.5 wt% SiO_2 , 76.9 wt% CaO , 5.7 wt% Fe_2O_3 , and 2.1 wt% MgO (Table 6).

The analysis of the ceramic matrix of Type 1 revealed a composition of 7.7–14.0 wt% Al_2O_3 , 28.8–40.1 wt% SiO_2 , 14.5–27.3 wt% CaO , 14.1–17.7 wt% Fe_2O_3 , and 8.4–28.1 wt% MgO , yet the presence of TiO_2 , K_2O , and P_2O_5 was also detected.

The analysis of the matrix of Type 2 revealed a composition of 7.7–16.2 wt% Al_2O_3 , 15.7–38.4 wt% SiO_2 , 24.7–66.4 wt% CaO , and 5.7–12.0 wt% Fe_2O_3 , yet the presence of TiO_2 , K_2O , MgO , and P_2O_5 was also detected.

The analyses of surfaces of both types showed areas in which lots of inclusions clustered together, according to BSE mode (Sample 2, Fig. 13c, two round particles; Sample 3, Fig. 14b, round dark particle; Sample 7, Fig. 16b, round particles). The Type 1 samples' inclusions revealed a composition of 3.7–4.3 wt% Al_2O_3 , 34.5 wt% SiO_2 , 6.5–7.0 wt% CaO , 11.0–16.5 wt% Fe_2O_3 , 0.4–0.9 wt% K_2O , and 37.9–42.8 wt% MgO (Table 6). Inclusions of Type 2 were not analyzed.

Table 5
Summary of Main Features of Petrographic Groups A and B Distinguished for Ashdod-Yam Roof Tiles.

Petro-fabric	A1	A2	A3	B	
Description	marl mixed with <i>terra rossa</i> pellets and dolomitic sand	marl mixed with <i>terra rossa</i> pellets and dolomitic sand	slightly silty marl with dolomitic sand	fine-grained marl with siliciclastic mudstones and detrital ophiolitic rocks	
Matrix	calcareous, pale yellowish/greenish gray in XPL and light brown in PPL; slightly optically active	calcareous, pale brown/greenish gray in XPL and light brown in PPL; non-optically active	calcareous, pale greenish gray in XPL and bright tan in PPL; slightly optically active	calcareous, yellowish tan in PPL, light yellow in XPL, speckled b-fabric; slightly optically active	
Voids	1 %; few micro-vesicles; oriented parallel to tile margin	1 %; few micro-vesicles; oriented parallel to tile margin	1 %; few elongated micro-vesicles; oriented parallel to tile margin	~1–3 %; mainly micro-vughs and micro-vesicles; oriented parallel and diagonal to vessel margin	
Sand-size non-plastic components	15–20 %; common poorly sorted euhedral rhomboid Dol (1–3 %, mode 70–200 µm); r/s-r nodules of fe.inc & fe.CP (<i>terra rossa</i>); 3–5 %, mode 100–400 µm); few s-r grains of micritic Lm (ca. 1 %, >400 µm), Sh fragments (>100 µm), Fe OP; very rare echinoderms; firing temperature above 750–800 °C	15–20 %; same as A1 for CF; see below difference for SF; firing temperature above 750–800 °C	10–15 %; same as A1 for CF, without fe.inc and with well-sorted euhedral rhomboid Dol (1–3 %, 100–200 µm); firing temperature above 750–800 °C	15–20 %; Md composed of dark red and orange peloid-like Hm, mud clumps and mud, Qz silt grains, and displacive needle-shaped Gy crystals (~3–5 %, >2.00 mm); a few Srp, eq (1 %, >150 µm), rare discrete detrital r & s-r micritic Lm (1 %, >200 µm); very rare s-ang & and s-r m.Qz; s-r & s-ang Cpx and Amph; firing temperature above 750–800 °C.	
Silt fraction	3–5 % of silty Qz of aeolian origin; Dol	1–2 % of silty Qz of aeolian origin; Dol	10–15 % of silty Qz of aeolian origin; Dol	1–3 % accessory minerals (Bt, Ms, Hbl, Pl, Ep, Zrn, Sps, Aug, and Srp)	
Samples	RT1, RT4, RT10, RT13	RT9	RT2, RT8	RT5, RT14	
Macro-fabric	YCW/RCW	YCW/RCW	YCW/RCW	YLW/RLW	
Type RT	<i>tegula</i> Type 2	<i>tegula</i> Type 2	<i>imbrex</i> Type 2	<i>tegula</i> Type 3	
Petro-fabric	C1	C2	C3	C4	D
Description	calcareous matrix with well-sorted ultra-basic magmatic rocks, temper	calcareous matrix with coarse ultra-basic magmatic rocks, temper	overfired calcareous matrix with ultra-basic magmatic rocks, temper	calcareous matrix with detrital sedimentary minerals and ultra-basic magmatic rocks	silty mud with alkali-feldspar and serpentine temper ("Nile" clay)
Matrix	calcareous; brown-orange XPL and PPL; low optical activity	calcareous; buff-orange to light brown; brown XPL and PPL; low optical activity	calcareous; light brown-buff in XPL and brown PPL; non-optically active	very calcareous; foraminiferous; slightly silty; dark brown in XPL and PPL; low optical activity	micaceous; dark reddish brown in XPL; dark brown in PPL; optically active
Voids	3 %; elongate meso-channels and meso-size vesicles and vughs; oriented parallel to vessel margins	5 %; mainly elongate meso-channels, meso- and macro-vughs; oriented parallel to tile margin	3 %; composed of mainly macro-vughs and meso-vesicles; oriented parallel to tile margin; micro-channeling	3 %; elongate macro-channels parallel to vessel margins and micro-channels surrounding voids	5 %; mainly elongate meso-channels and meso-macro vughs; micro-channeling multiple orientations
Sand-size non-plastic components	25–30 %; dominant ol/idd (generally ang & s-r, mode 200–400 µm); common Srp (generally ang & s-ang, mode 100–200 µm); coarse s-r CP (mode 200–400 µm); few eq & s-ang Pl (mode 100–200 µm); rare Chl (<150 µm); few-very few hbl, Qz, ch, cpx (<100 µm); rare-very rare p.Qz, kfs, bt, opx (<1 %, <100 µm)	25–30 %; similar to C1 but poorly calibrated crushed ferromagnesian temper added to clay recipe (eq & s-ang ol/idd, Srp, Pl, Cpx, & Opx)	15 %; CF similar in size and sorting to C1, although quite affected by firing, with high grade of dissociation of cal incl.	15–20 %; dominant cal incl. and cal.mf (generally s-ang & sr, mode 100–400 µm); few ang & s-ang srp/idd (mode 200–300 µm); few-very few hbl (<100 µm), Qz (<200 µm), ch (<60 µm), cpx (<100 µm); rare-very rare pl, p. Qz, kfs, bt, opx (<50 µm); common presence of burned-out vegetal temper (3–5 %, >2.00 mm)	25–30 %; common poorly sorted coarse s-ang & Qz coated with Cal.c and Kfs (200–1000 µm); ang. s-r Srp (100–200 µm); rare s- and Pl (100–150 µm); common Mu (mode 100–300 µm); few Mc (400 µm); very rare elongated s-r Bt (<200 µm)
Silt fraction	<1–2 %; scarce; mainly Qz with few Zrn, Ms, and Hbl, ol, pl, cpx, kfs, fe.inc, srp, p.Qz, hbl, bt, ch, Ep	<1–2 %; same as C1	<1–2 %; same as C1; burned cal inc.	<1–2 % scarce; mainly cal.mf, cal inc., Ca, Qz, Zrn, Ms, Hbl, ol, pl, cpx, kfs, fe.inc, srp, p.Qz, hbl, bt, ch, Ep	<15–20 %; predominant Mu; abundant ang Qz, Bt; few Kfs, Hbl, Zrn, Cpx, and Ep
Samples	RT3	RT6, RT7, RT12	RT11	RT16	RT17
Macro-fabric	LOW	LOW	LOW	LOW	other
Type	<i>tegula</i> Type 1	<i>tegula</i> Type 1	<i>tegula</i> Type 1	<i>tegula</i> Type 1	other

Notes: A detailed description of the different fabric groups can be found in the supplementary information. Categories for the frequency of inclusions are based on Whitbread (1995). Abbreviations for rock-forming minerals (based on Kretz, 1983): Amph = amphiboles, Aug = augite, Bio = biotite, Ca = calcite, cal = calcareous, cal.mf = calcareous microfossils, CP = clay pellets, Chl = chlorite, Ch = chert, Cpx = Clinopyroxene, Dol = Dolomite, Ep = epidote, Fe.inc = ferruginous inclusions, Gy = gypsum, Hbl = hornblende, Hm = hematite, idd = iddingsite, K-FS = feldspar, Lm = limestone, Md = Mudstone, Mc = microcline, Mu = muscovite, Ol = olivine, OP = opaque, Opx = orthopyroxene, p.Qz = polycrystalline quartz, m.Qz = monocrystalline quartz, Pl = plagioclase, Qz = quartz, Sh = shales, Srp = serpentine, Zrn = zircon; r = rounded, ang = angular, s- = sub, CF = coarse fraction, SF = silt fraction.

Table 6
SEM-EDS chemical analysis of ceramic substrate of roof tiles covered with mortar remains and paint.

Sample	Composition Weight Percentage (wt.%)								
	Al ₂ O ₃	SiO ₂	CaO	Fe ₂ O ₃	TiO ₂	K ₂ O	MgO	MnO	P ₂ O ₅
Red Pigment									
Sample 1 (Type 1 RT), area of red pigment (P-CS, Fig. 12b), SA: 400 μm × 400 μm	9.6	24.9	26.9	27.8	–	1.4	9.4	–	–
Sample 1 (Type 1 RT), area of red pigment (P-CS, Fig. 12d), SA: 30 μm × 30 μm	4.3	10.5	10.5	71.4	–	–	3.3	–	–
Sample 2 (Type 1 RT), ceramic substrate and red pigment (P-CS, Fig. 13a, inside square), SA: 500 μm × 500 μm	10.5	30.5	21.4	17.7	–	2.0	17.9	–	–
Sample 2 (Type 1 RT), area of red pigment (P-CS, Fig. 13b), SA: 250 μm × 250 μm	7.1	12.1	12.3	64.9	–	0.6	3.0	–	–
Sample 3 (Type 2 RT), red pigment particles (P-CS, Fig. 14b, Area 1 and Fig. 9c), SA: 250 μm × 250 μm	7.8	16.5	46.8	23.3	1.3	1.5	2.8	–	–
Sample 4 (Type 2 RT), red pigment (P-CS, Fig. 15c, Area 1 and Fig. 10d), SA: 50 μm × 50 μm	12.5	19.7	17.5	46.0	–	0.8	3.5	–	–
Sample 4 (Type 2 RT), red pigment (P-CS, Fig. 15c, Area 2), SA: 50 μm × 50 μm	7.7	20.6	52.3	11.2	1.9	2.1	4.2	–	–
Sample 7 (Type 1 RT), red pigment (P-CS, Fig. 16b, Area 1 and Fig. 9c), SA: 60 μm × 60 μm	6.2	14.5	9.4	63.4	–	1.2	3.0	2.3	–
Black Pigment									
Sample 4 (Type 2 RT), black pigment (P-CS, Fig. 15c, Area 3 and Fig. 10e), SA: 150 μm × 150 μm	4.8	10.5	76.9	5.7	–	–	2.1	–	–
Ceramic Stratum									
Sample 1 (Type 1 RT), area of ceramic substrate (P-CS, Fig. 12c), SA: 400 μm × 400 μm	14.0	40.1	14.5	14.2	0.9	3.3	12.1	–	0.9
Sample 2 (Type 1 RT), area of ceramic substrate with cluster of inclusions (P-CS, Fig. 13c, inside square), SA: 1000 μm × 1000 μm	7.7	28.8	19.9	14.1	–	1.0	28.5	–	–
Sample 3 (Type 2 RT), area of ceramic substrate (P-CS, Fig. 14b, Area 2), SA: 250 μm × 250 μm	7.7	15.7	66.4	5.7	–	1.4	3.1	–	–
Sample 3 (Type 2 RT), ceramic substrate (P-CS, Fig. 14b, Area 3), SA: 250 μm × 250 μm	12.6	30.0	39.4	8.0	–	2.0	6.9	–	1.1
Sample 3 (Type 2 RT), of ceramic substrate (P-CS, Fig. 14b, Area 4), SA: 250 μm × 250 μm	15.0	33.1	35.1	8.6	0.9	5.7	1.6	–	–
Sample 4 (Type 2 RT), ceramic substrate (P-CS), SA: 250 μm × 250 μm	16.2	38.4	24.7	12.0	2.0	4.0	2.7	–	–
Sample 7 (Type 1 RT), ceramic substrate (P-CS, Fig. 16b, Area 2, and Fig. 11d), SA: 100 μm × 100 μm	11.4	32.1	27.3	17.7	1.2	1.9	8.4	–	–
Inclusions									
Sample 2 (Type 1 RT), cluster of inclusions (P-CS, Fig. 13d), SA: 250 μm × 250 μm	4.3	34.5	6.5	11.0	–	0.9	42.8	–	–
Sample 2 (Type 1 RT), area of ceramic substrate with cluster of inclusions (P-CS, Fig. 3c, inside square), SA: 1000 μm × 1000 μm	7.7	28.8	19.9	14.1	–	1.0	28.5	–	–
Sample 7 (Type 1 RT), cluster of inclusions (P-CS, Fig. 16b, Area 3), SA: 80 μm × 80 μm	3.7	34.5	7.0	16.5	–	0.4	37.9	–	–

Note: SA represents the scanned area.

5. Summary of main results

This multidisciplinary analysis aimed at the compositional, microstructural, and mineralogical characterization of the roof tiles and pigments. The results reveal a distinct correlation among the identified types, macro-fabrics, and petro-fabrics:

Group 1, LOW, which is typologically Type 1, matches with Petro-group C. TSPA showed that the clays used in producing Petro-fabrics C1–C4 were sourced in ophiolitic complexes originating in the north-eastern Mediterranean. Ophiolitic clays were commonly used as a raw material for pottery production in the eastern Mediterranean (Degryse et al., 2003) and were exchanged extensively throughout the Mediterranean basin in the *longue durée*. The use of ophiolitic clays has already been documented for Roman and Byzantine roof tiles in Beirut (Mills, 2013), Ashqelon (Cohen-Weinberger et al., 2024), and Caesarea Maritima (Bouzaglou, forthcoming). A key difference between the Mediterranean region ophiolites would be the respective rock compositions, which differ depending on location and the local specific formative tectonic processes. However, the lack of systematic quantitative petrographical analyses and geochemical characterization, as well as our difficulty in reconciling both datasets, precludes our ability to define markers and to pinpoint clear CBM production centers. This technical difficulty not only testifies to the limitations of the existing methodological frameworks but also limits our ability to accurately estimate the prevailing exchange networks and thus to evaluate each region's role in producing ceramics. Our mineralogical estimation is thus restricted to a Mediterranean origin in a triangle located between Cyprus, Cilicia, and northern Syria. While no morphological parallels have been published from these regions, their petrography suggests eastern Cilicia to be the most likely place of origin (Bes and Braekmans, forthcoming). INAA performed on two samples yielded inconclusive results. Additional geochemical analyses of ophiolitic-based ceramics are required to determine their specific origins.

Group 2, YCW/RCW, corresponding to typology Type 2, is identified with Petro-group A. The tiles in this group are defined by their buff-yellow to buff-reddish color and a very hard fabric. The consistent use

of Moza unit clays indicates a Judean Hills sourcing. Comparing the roof tiles from the Jerusalem Convention Center (Cohen-Weinberger et al., 2017, Group A; 2020, Groups A and B) with those under discussion in this paper shows a notable lithological resemblance among the samples. While the petrographic analysis does not pinpoint a clear production center within the Moza unit, the chemical analysis of one roof tile does indicate that Petro-fabric A1 (see supplementary material) originates in the Hebron region, some 30 km south of Jerusalem. This group, labeled HebA, was already well identified in ceramic wasters from the Iron Age and the Early Roman period unearthed at Tel Hebron (Ben-Shlomo, 2020:Fig. 8; Ben-Shlomo and Mommsen, 2018, 2019). Notably, Tel Hebron is situated atop Moza clay deposits, with petrographic analysis showing a prevalent silty dolomite component in most specimens (Ben-Shlomo 2020:98–100 [Groups 1 and 2]). Therefore Petro-fabric A1 may represent a Hebron-area version of Moza clay (Ben-Shlomo and Mommsen, 2019:218). Group A's production was thus either in Hebron close to the source or in or around Jerusalem, where most of the roof tiles discussed here were found. The Moza clay sources around Jerusalem, however, might be geochemically similar and may also represent possible sources. An additional sample associated with Petro-fabric A3 (see supplementary material) produced inconclusive results, possibly because of its composite structure. This sample exhibited streaks of calcareous clay in varying colors, suggesting the mixing of clays identified through TSPA.

Group 3, YLW/RLW, which aligns with typology Type 3, is associated with Petro-group B. This group comprises lightweight roof tiles of a soft fabric. Their provenance was tentatively attributed to Cyprus on petrographic grounds and then morphologically confirmed by already documented and published “yellow tiles” from the region (Rautman et al., 1993:Fig. 3.22). The INAA results, however, were inconclusive.

Based on SEM-EDS analysis results, the red paint on Type 1 RTs revealed the presence of 27.8–71.4 wt% Fe₂O₃. The red paint on Type 2 tiles revealed the presence of 11.2–46.0 wt% Fe₂O₃, which is much higher than the ceramic substrate iron oxide concentration (Table 6). Therefore the surface red paint was identified as ochre pigment. Based on the EDS analysis composition of Type 2 tiles' black paint, with low

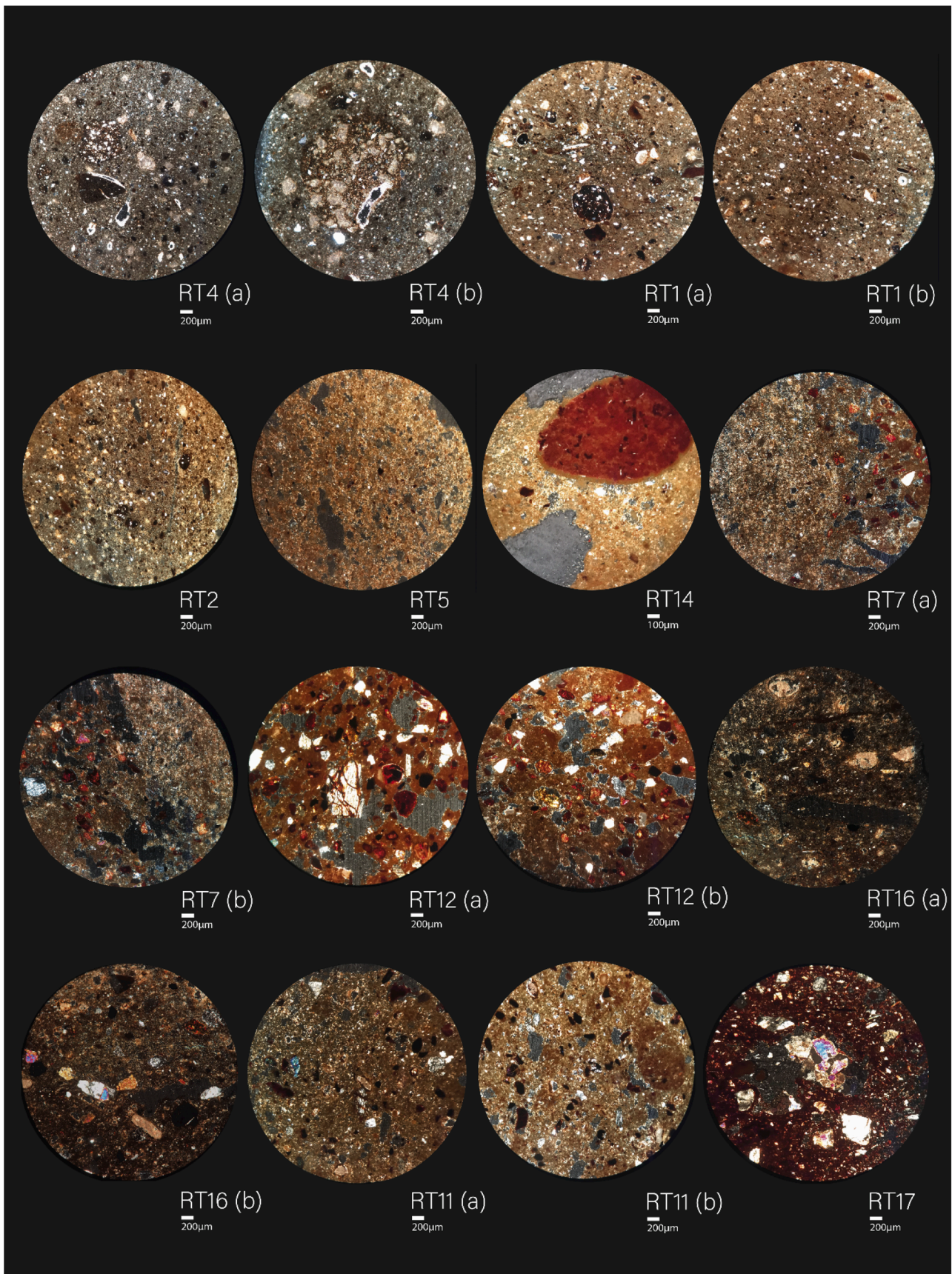


Fig. 9. Thin section pictures (Petro-fabric A: RT1, 2, and 4; Petro-fabric B: RT5 and 14; Petro-fabric C: RT7, 12, 11, and 16; Petro-fabric D: RT17). Photographs were taken under cross-polarized light (photos by Liora Bouzaglou).

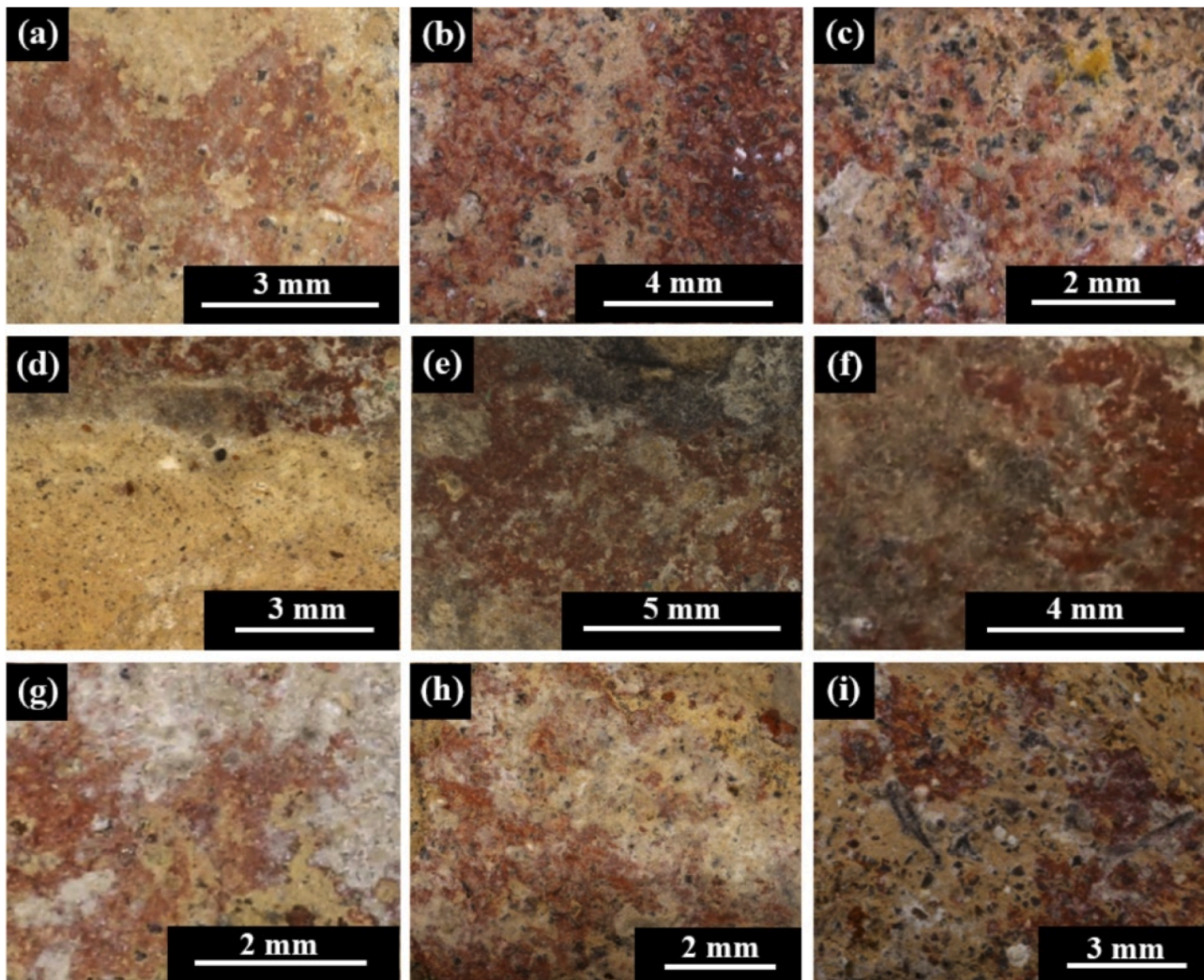


Fig. 10. A catalog of Byzantine roof tile ceramics and pigments retrieved from Ashdod-Yam: (a) Sample 1 (imported RT, Type 1), with red paint on top (P-section); (b) Sample 2 (imported RT, Type 1), ceramic matrix mixed with dark mineral particles (temper) and red paint covered with small remnants of white mortar (P-section); (c) higher magnification of Sample 2's surface showing ceramic mixed with temper, covered with white mortar and red and yellow paint (P-section); (d) Sample 3 (local/regional RT, Type 2), layered structure of ceramic substrate covered with red pigment (T-CS); (e) Sample 3 (local/regional RT), ceramic material covered with white mortar and red and black paint (P-section); (f) Sample 4 (local/regional RT, Type 2), with red and black paint (P-section); (g) Sample 5 (imported RT, Type 1), with white mortar, red paint, and ceramic material beneath it (P-section); (h) Sample 6 (imported RT, Type 1), with white mortar and red paint on top and a ceramic substrate beneath it (P-section); (i) Sample 7 (imported RT, Type 1), with red paint and remains of white mortar and beneath it a ceramic matrix mixed with dark temper (P-section) (photos by Dana Ashkenazi; Canon 6D camera).

iron oxide concentration (5.7 wt% Fe_2O_3), the presence of elements similar to the ceramic substrate, and the dark area observed by SEM BSE mode observation, it is almost certainly identified as carbon black pigments mixed with calcium carbonate mineral (Ashkenazi et al., 2021). Similarly, micro-XRF analysis on one painted roof tile from Jerash revealed the use of two different pigments, red and black, made respectively from iron oxides and carbon mixed with calcium (Ebeling and Barfod, 2022).

6. Discussion

6.1. Production technology

Based on VT inspection, camera photos, stereomicroscope observation, SEM observation in SE and BSE modes, and TSPA, it was determined that Type 2 roof tiles are finer, contain fewer micro-vesicles, and demonstrate greater homogeneity than Type 1 samples. The latter exhibited numerous elongated channels as well as meso-vughs and vesicles. These disparities may be attributed to the clay homogenization

process. Type 1/Petro-group C showed elongated voids between clumps of clay, indicative of inadequate paste blending before molding and insufficient homogenization. This inadequate homogenization is observable in the stratification of two clay slabs, one free of aplastic inclusions and the other containing ophiolitic inclusions (Fig. 8, RT7). Such voids could also result from the folding of clay during kneading, trapping air that manifests as pores or voids in the fired product (Quinn, 2022:81). Also, the mixture of subrounded and subangular grains of ferromagnesian silicates is averagely to poorly calibrated.

In contrast, Type 2/Petro-group A was more thoroughly homogenized, exhibiting fewer voids. The presence of discrete differently colored marble structures within the matrix suggests the mixing of clays, which enhances the workability and firing performance of the individual clays (Eramo, 2020:163–64; Whitbread, 1995). *Terra rossa* soil, once dried and powdered, was combined with marl to enhance the clay's quality. This addition enabled the tiles to achieve sintering at comparatively low temperatures (Quinn, 2022:230; Rice, 2015:13) and also reduced the clay's plasticity (Cohen-Weinberger and Goren, 1996: 81). The presence of silt-size quartz within the nodules suggests that the

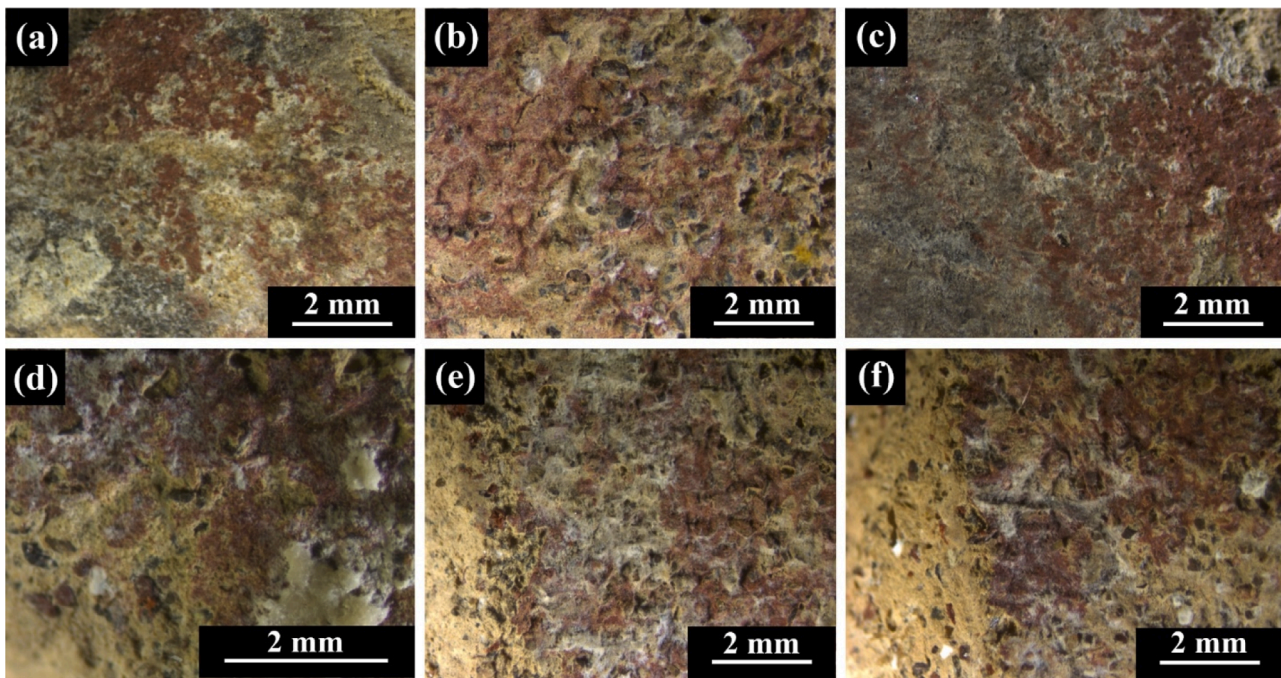


Fig. 11. Stereomicroscope images of Byzantine roof tile ceramics and pigments: (a) Sample 1 (imported RT, Type 1), covered with red paint and some black areas (P-section); (b) Sample 2's surface (imported RT, Type 1), showing ceramic matrix mixed with black temper, covered with areas of white mortar material and red and yellow paint (P-section); (c) Sample 4 (local/regional RT, Type 2), with red and black paint (P-section); (d) Sample 5 (imported RT, Type 1), showing ceramic matrix mixed with black temper, covered with white mortar and red paint (P-section); (e) Sample 6 (imported RT, Type 1), ceramic material covered with white mortar and red paint (P-section); (f) Sample 7 (imported RT, Type 1), ceramic matrix (left side of image) mixed with black temper, covered with white mortar and red paint (P-section) (photos by Dana Ashkenazi; Discovery V8 Zeiss instrument).

powdered clay remained dry during the paste's wetting and tempering process.

Similarly, Type 3/Petro-group B used mudstone temper. This approach is typically employed for large to medium-size, thick-walled, hand-formed vessels. Adding mudstone allows the diminution of the clay's plasticity and prevents cracking during drying (Makarona et al., 2016). Moreover, the objects' bright color and lightness may have been achieved by mixing seawater—rich in sodium and carbon from the salt—into the clay. Alternatively, adding salt, a practice common among traditional potters in Italy and Sicily (Hampe and Winter, 1965:176), could serve to expedite the drying process and to impart either a bright yellow color at high firing temperatures or a bright red color at lower temperatures.

Rautman et al., (1999) examined Late Roman-period roof tiles from Cyprus, determining that although the larger tiles composed of coarse clay mixtures were made locally, the smaller, higher-quality tiles were manufactured in specific areas of Cyprus and then distributed to other regions via maritime transport (Eiland and Williams, 2001; Rautman et al., 1999).

Regarding the Ashdod-Yam church, a contrasting scenario emerges when comparing the Type 2 roof tiles produced in the Judean Hills to the Type 1 Cilicia/Cyprus imports. Although Type 1 roof tiles are characterized by a coarse clay mixture, *coarse* does not mean lower quality. In fact, incorporating coarse temper from ophiolitic regions into the raw material could actually confer enhanced durability to the roof tiles.

The intentionally added ultra-basic magmatic and volcanic rock tempers are a common ingredient of CBM and of specialized coarse wares such as *mortaria*, *dolia*, and basins (Blakely et al., 1992:208, 215). Key physical properties of ophiolitic-based clays are their plasticity, high shrinkage rate, and low porosity. Ultra-basic magmatic rocks have a greater thermal expansion coefficient than typically low-fired clay minerals, which are known to cause microdamage around temper particles during firing (Sultana et al., 2015). Consequently, adding ophiolitic rocks into the tile paste improved the behavior of water absorption

and overall mechanical strength while also allowing for a lower shrinkage value and facilitating demolding (Müller, 2017:616), sought-after properties for roof tile production.

While ceramic production is well-known in the Ashdod region and pottery workshops were notably documented for the Byzantine period (Baumgarten, 2000), the local geology and lithology may not have been suitable for CBM production. Although *hamra* (reddish clayey sand or loam) constitutes the southern coastal plain's main outcrop and is indeed an appropriate choice for pottery and sun-dried brick manufacture (Bakler, 1982:65–66; Lorenzon et al., 2023), this material fails to fulfill CBM requirements. Nor is the dark brown clayey soil found in floodplain and young valley alluvium usable. Furthermore, a common trait for all petro-groups identified is the use of marl as a clay base, as it has a high level of plasticity, good workability, resistance to high temperatures, and a fine-grained texture. Above all, marl has good water retention properties due to its high clay content, such that firing at high temperatures creates a dense, nonporous surface resistant to water absorption. However, this type of soil was unavailable here. Another factor seemingly contributing to local CBM production's absence is that fuel for the kilns was likely as sparse in the Ashdod region as it is today, needing to be imported and thus raising production costs. Azotos Paralios, among other Levantine coastal cities, therefore imported the materials necessary for constructing its urban and religious landscape.

6.2. Ashdod-Yam roof tiles in context: a regional coastal site analysis

The simultaneous use of two roof tile types with two distant sources, a northeastern Mediterranean type used side by side with a Judean Hills type, at a single site and on the same building, without any evidence of local production, is not an isolated occurrence in the southern Levant.

Northeastern Mediterranean roof tiles are evidenced at various coastal locations, such as Khirbet Barqa (near Ashdod), Caesarea

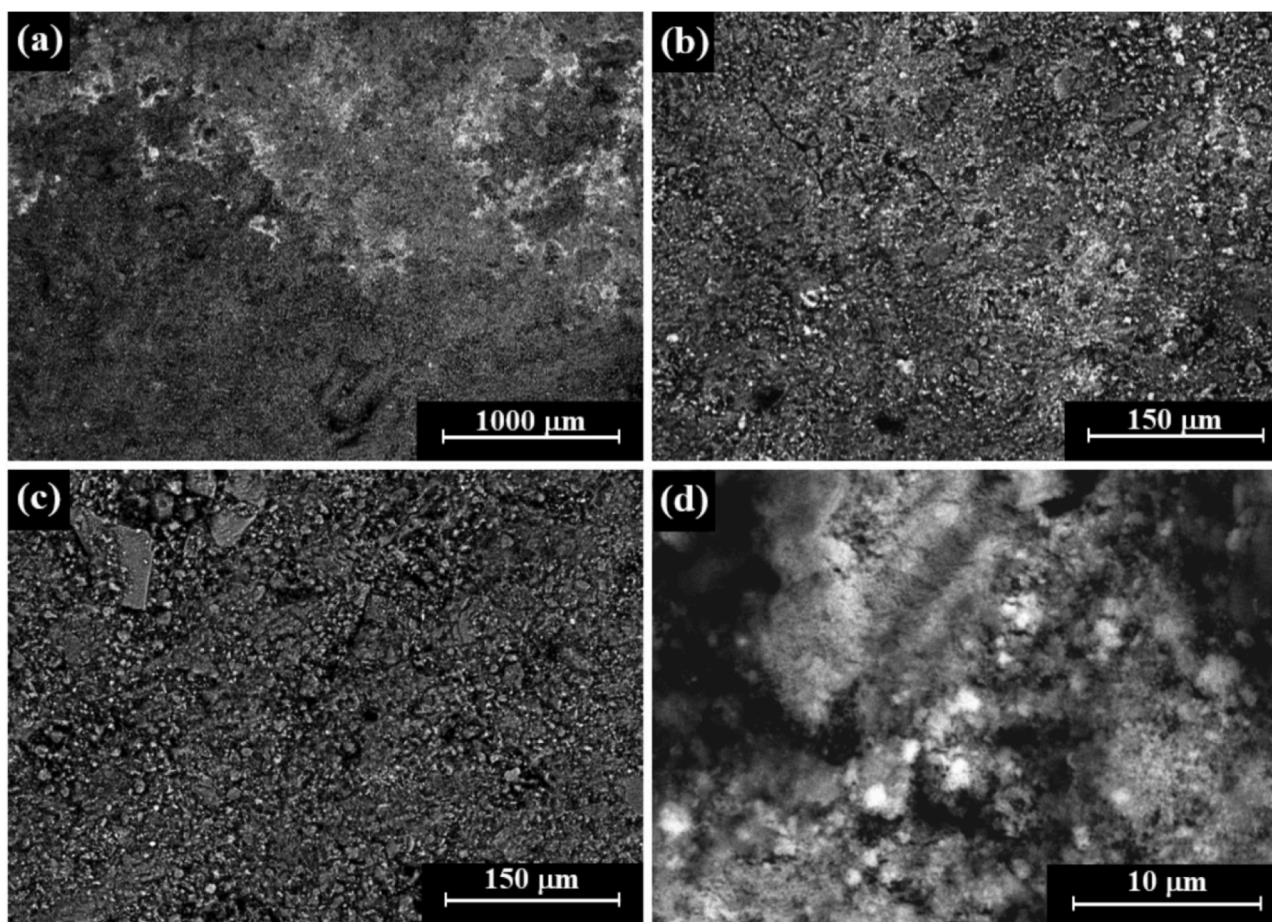


Fig. 12. SEM images of Sample 1's ceramic substrate (Type 1 RT), covered with red paint (P-section, BSE mode): (a) general view of the surface showing dark and bright areas; bright areas are rich with red pigment particles; (b) higher magnification of the bright area; (c) higher magnification of the dark area; and (d) higher magnification of the bright area shown in Fig. 12b.

Maritima, Tel Keisan, and Nahariya.^b The roof tiles found in the church of Khirbet Barqa, between Gan Yavne and Ashdod, in particular share a history and fate with those of Ashdod-Yam. This building was also destroyed by fire and in the same period, at the end of the sixth century CE. Here too a destruction layer, mostly featuring roof tiles atop a mosaic floor, was partially preserved upon excavation (Rapuanò, 2016:117–18, Fig. 1.1–12; Sion, 2016). Similarly, the roof tiles documented from Tel Keisan and Nahariya were recovered from Byzantine churches (Dauphin and Edelstein, 1984:15–25, Fig. 2C-72/10, 46–47; Landgraf, 1980) and retrieved from primary deposits, just as at Ashdod-Yam and Khirbet Barqa.

The Khirbet Barqa tiles appear to be of Type 1, thus likely belonging to Petro-group C, based on their form. The Tel Keisan roof tiles are morphologically consistent with Type 1/Petro-group C and Type 3/Petro-group B from Ashdod-Yam. The Nahariya *imbrices* numbered C-78/46 and 47, only depicted in drawings and lacking any descriptive detail, seem to match the form of Type 3/Petro-group B from Ashdod-Yam. A potentially parallel situation arises at Tel 'Afar, where numerous imported roof tile fragments were discovered, dislocated from their original context. Peilstöcker's (2009:111–13, Figure 11.4) Type 1

^b The roof tiles of Khirbet Khaur el-Bak and Ashqelon were dated to the Roman period and are morphologically distinct from those of Ashdod. Thus they are excluded from further discussion here (Cohen-Weinberger et al. 2024). However, it should be pointed out that the general color and shape of the published *imbrices* are similar to those from the church of Ashdod-Yam (Cohen-Weinberger et al. 2024:Figure 5.3–4).

roof tile there is identified with our Type 1/Petro-group C, based on morphology. These *tegulae* likely eroded down the tel and originated from a “monumental building” atop it, which may have also been a church.

A similar situation of combining materials from differing sources is observed in Caesarea. A significant portion of the CBM, particularly roof tiles, was imported from the northeastern Mediterranean, while only a small number of items, such as *tubuli*/box flue tiles, were produced locally (Bouzaglou, forthcoming, with petrography [import from Cyprus]; Peleg and Reich, 1992:155, Fig. 17, morphologically identified as Type 1/Petro-group C, potential from Cilicia).

In the case of Khirbet Barqa, located in Ashdod's general vicinity, while its church's destruction debris was less complete in comparison to Ashdod-Yam, all the surviving roof tiles were imports. That in each site a significant number of roof tiles likely came from the northeastern Mediterranean raises questions about whether local production existed in Ashdod-Yam and its surroundings, as no locally produced roof tiles have been found. Similarly, evidence from Tel Keisan and Nahariya also points to a lack of local production. Roof tiles at these two large centers close to the sea were all imported from either the northeastern Mediterranean, including Cyprus. Not only was their production center not local, but their imports did also not even originate in the closest metropolis, Akko-Ptolemais (Acre), which suggests that it did not produce roof tiles either. Consequently, the prevalence of northeastern Mediterranean roof tiles in Tel Keisan, Nahariya, Tel 'Afar, and Khirbet Barqa, as well as in larger hubs like Ashdod-Yam and Caesarea Maritima, may be attributed not just to the presumed stylistic preferences of these communities but also point to the total absence of local manufacturing

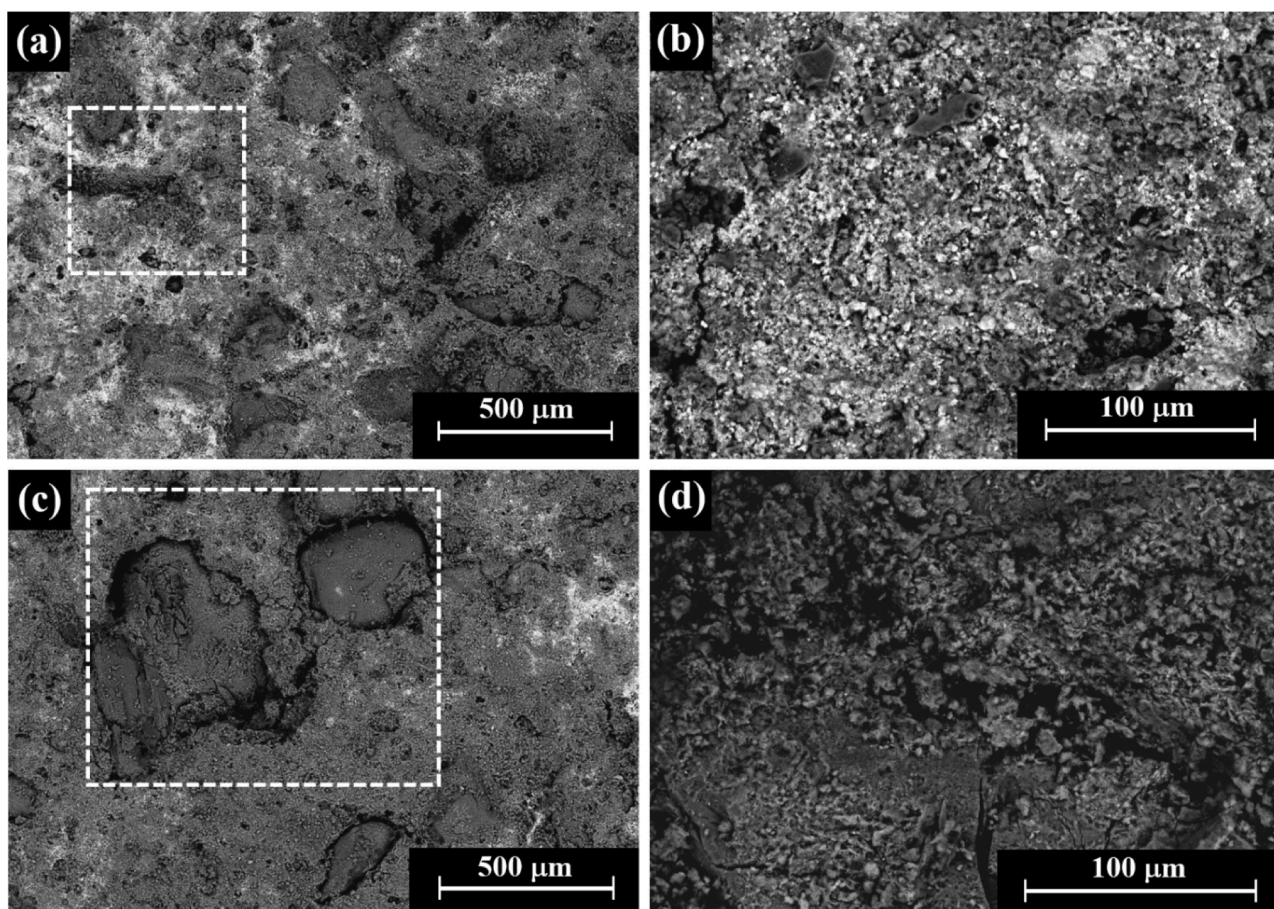


Fig. 13. SEM images of Sample no 2's ceramic substrate (Type 1 RT), covered with red paint (P-section, BSE mode): (a) general view of bright and dark areas; bright areas are rich with red pigment particles; the area inside the square was examined by EDS analysis; (b) red pigment particles; (c) ceramic material mixed with three mineral particles (temper); the area inside the square was examined by EDS analysis; (d) area inside a typical temper particle (photos by Dana Ashkenazi).

options. This may partly be due to the dearth of appropriate raw materials, as suggested above.

Support for the northeastern Mediterranean's significant role in supplying roof tiles is also discernible in the vicinity of Cyprus, particularly by their presence in cargoes preserved in shipwrecks near Cape Andreas, at the island's northeastern extremity (Green, 1971, 2019). It is important to note that these roof tiles have not undergone petrographic analysis. Morphologically, though, some are indeed identified as similar to Ashdod-Yam Type 3/Petro-group B Cypriot imports (Green, 1971: Figs. 24–25).

To review, the modest but significant collection of northeastern Mediterranean roof tiles found in several coastal sites is indicative of the pivotal role regions such as Cyprus and Cilicia played in supplying roof tiles to the southern Levant's coast and potentially to other regions as well. Maritime transport from the northeastern Mediterranean proved to be more economical than overland routes (Adan-Bayewitz and Perlman, 1990:158; Bresson, 2016:84–88; Casson, 1974:150–51, 170–71), likely influencing the prevalence of fully imported roof tile assemblages.

While the above argument does account for the presence of northeastern Mediterranean roof tiles (Type 1/Petro-group C) by the mechanisms of offer/demand/logistical efficacy, the presence of Type 2/Petro-group A tiles demands another explanation. They are identified as coming from the Judean Hills (possibly from the Hebron or Jerusalem regions), and the coastal city of Ashdod-Yam is located far beyond the limits of their main usage area: Jerusalem itself and its immediate vicinity, as well as the Judean Desert and parts of the Shephela. (See the list of find spots above.) These CBM-producing workshops were plausibly situated near Jerusalem to meet the burgeoning demand for

ceramic building materials driven by this period's intense construction activity. Materials were thus assumedly manufactured, procured, and transported to serve local construction needs. Whatever purpose or feature the distant Ashdod-Yam congregation saw in them must have justified the costs and risk of overland transport.

Hypothetically, quality could have played this role; the Jerusalem-area roof tiles were much harder fired and thus were potentially seen as being of higher quality and durability. Another driving factor could have been Jerusalem's high status in Christianity. Referencing the Holy City's skyline familiar to pilgrims would visually prompt associating this church with Jerusalem. A third factor could lie in the fact that, as shown below, some roof tiles employed here were in secondary usage. Perhaps some of these were from Jerusalem and the congregation purchased more of the exact same type in an attempt to create a uniform roof. A last factor might have been availability: The Jerusalem-region roof tiles were mostly found within the earlier main nave, while those from the northeastern Mediterranean were retrieved from the later-added annexes. One of the two suppliers might have not been available and an alternative source was needed as either the main nave or the annexes were being finished.

6.3. Assessing ocher pigment presence

Initially two options were considered to explain the presence of red painted lines on the top of tiles from various provenances: the pigments could have been prepared and applied at the roof tile production centers, or the tiles were first painted on-site at the church. Furthermore, the purpose of painting the tiles invites conjecture: the paint could have

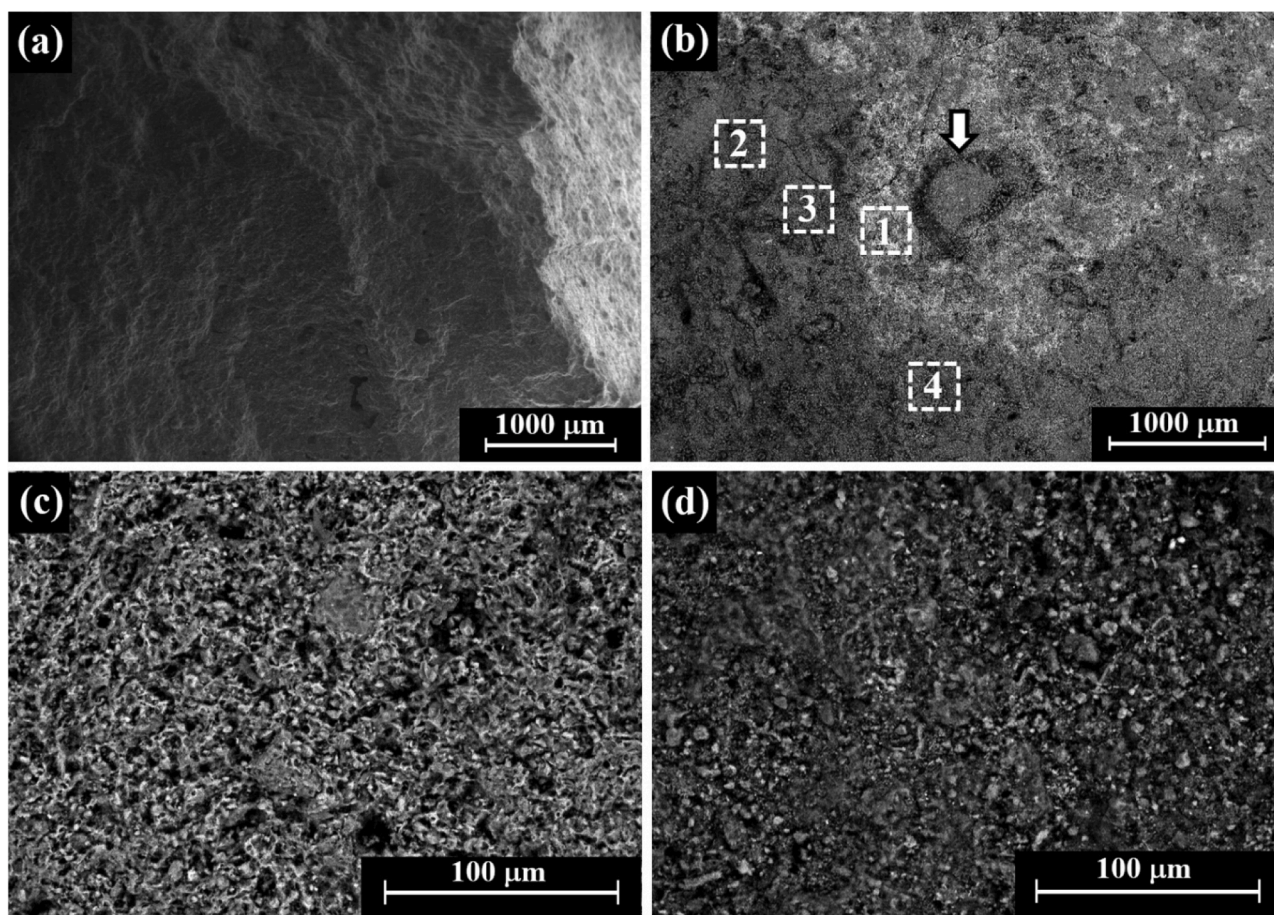


Fig. 14. SEM images of Sample 3's (Type 2 RT) ceramic substrate, covered with red paint (P-section): (a) general surface topography view (SE mode); (b) general view of dark ceramic areas, bright area rich with red pigment particles, and a temper (arrow) at center of image (BSE mode); areas inside the squares were examined by EDS analysis; (c) higher magnification of the bright red pigment particles shown in Fig. 14b; Area 1 examined by EDS (BSE mode); (d) higher magnification of the dark area shown in Fig. 14b; area 4 examined by EDS (BSE mode) (photos by Dana Ashkenazi).

served during construction as a maker's mark signifying church ownership, or it could have been intended for aesthetic and visual enhancement.

By considering the similarity of the natural pigments found on top of both Types 1 and 2 at Ashdod-Yam in terms of colors, compositions, and microstructures, and especially considering their respective distant provenances of tile manufacture, it is now certain that the pigments were produced regionally (if not locally) and were applied to the roof tiles only during the construction process. Hence they share similarities, despite being found on tiles with different places of origin. Furthermore, their colors, composition, and microstructure are similar to those of other regionally discovered archaeological paints (Ashkenazi et al., 2021; Ebeling and Barfod, 2022).

The horizontally and straight drawn lines, as well as the bands, were always parallel to the upper end and lines of mortar (Fig. 4). They were therefore probably intended to mark the desired overlap (maximum or minimum) of two *tegulae* and *imbrices*. This is also suggested by the consistent distances of the lines, as well as the mortar, from the upper end and may have marked and guided the proper application of mortar as well. In addition to that, the lines helped maintain the consistent horizontal structure of the roof tiles during the roofing process, reasonably necessitated when combining morphologically different types of tiles. Therefore the composite nature of the roof, the chemical uniformity of the pigments and the consistent parallel presence of mortar all suggest that the paint was applied during the roof's construction, a method so far undocumented for the Byzantine period.

Earlier we raised the seeming contradiction between evidence of

fully painted tiles as opposed to traces of distinct painted lines, which seemed mutually exclusive since assumedly lines of the exact same color would not be applied to fully painted tiles. Yet it was noted that the traces of lines were mostly well preserved but the remains of potentially completely red-painted surfaces were not. This physical evidence and the incoherency of the two possible intentions of color application suggest that possibility that at times there were one or more older layers of color on a tile. This interpretation also allows for the equally badly preserved remains of black color to fit within the rest of the evidence—the black spots are the remains of an older paint application. Thus it is very likely that some of the church's top roof tiles, deposited within the same destruction event, were previously used on other roofs; hence their paint was faded. Upon reuse in this church's construction, they were freshly painted with red lines, which easily stood out despite the older paint layer. The red lines served the construction process for the reasons suggested above and possibly addressed other, more complicated motives as well.

7. Conclusions

This multi-analytical approach draws on typology, macroscopic observations, ceramic petrography, geochemistry, and scanning imagery evidence to explore roof tile production, distribution, and consumption at Ashdod-Yam between the late fourth/early fifth century CE and the late sixth century CE. Owing to its geographical position bridging the Mediterranean Sea and the Byzantine-period province of Palaestina Prima, the Ashdod-Yam church's repertoire of roof tiles was completely

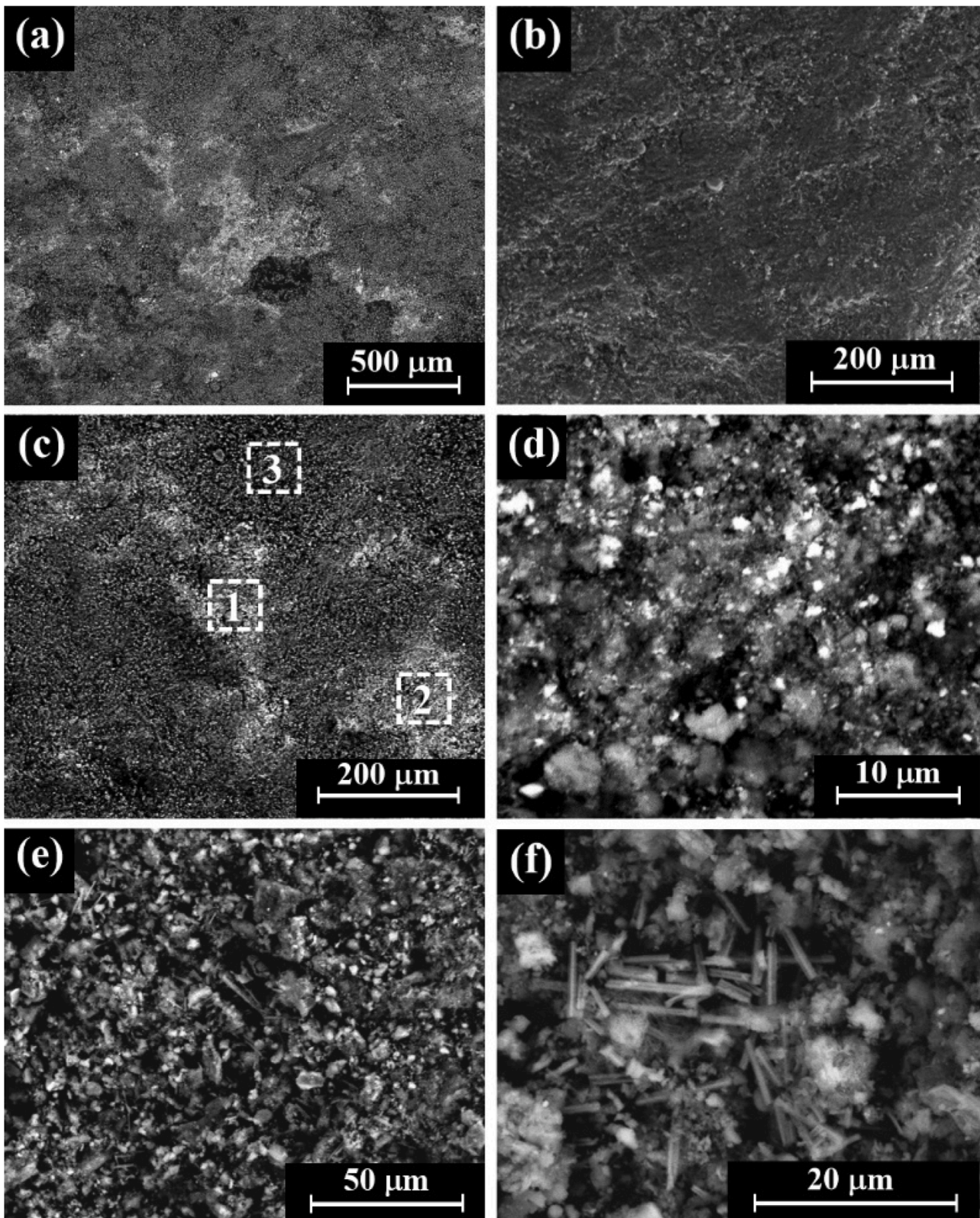


Fig. 15. SEM images of local/regional Sample 4's ceramic substrate (Type 2 RT), covered with red and black paint (P-section): (a) general view of bright and dark areas; bright areas are rich with red pigment particles; dark area at image's upper part contains black paint (BSE mode); (b) surface topography (SE mode); (c) dark ceramic areas and bright areas rich with red pigment particles (BSE mode); areas inside squares were examined by EDS; (d) higher magnification of bright red pigment particles shown in Fig. 15c; (e)–(f) higher magnifications of dark Area 3 shown in Fig. 15c, covered with black paint (photos by Dana Ashkenazi).

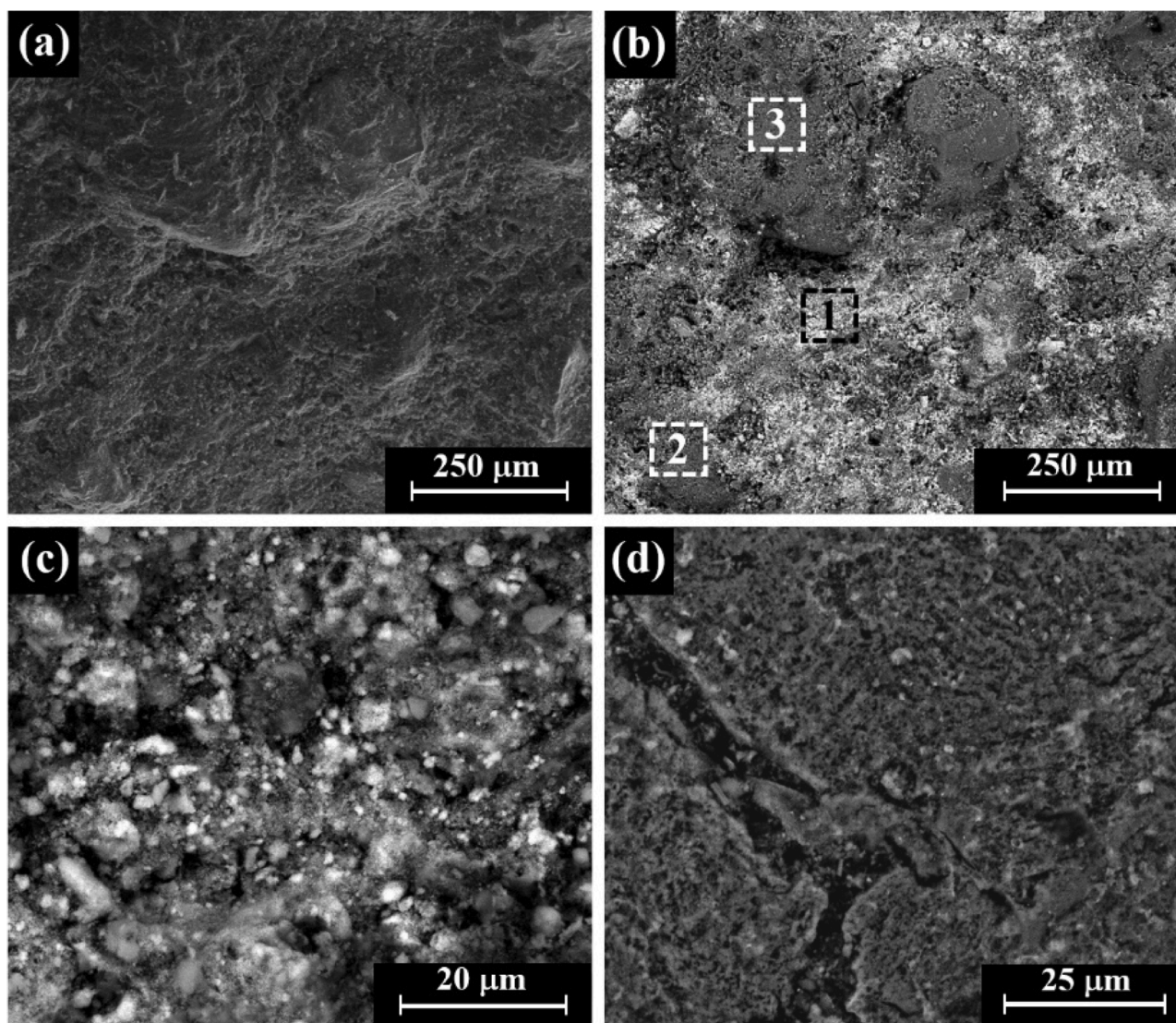


Fig. 16. SEM images of Sample 7 (Type 1 RT, P-section, BSE mode): (a) view of surface topography (SE mode); (b) bright and dark areas; bright areas are rich with red pigment particles; (c) higher magnification of bright red pigment particles (Fig. 16b, Area 1); (d) higher magnifications of the ceramic material shown in Fig. 16b, Area 2 (photos by Dana Ashkenazi).

imported, originating both from the northeastern Mediterranean—Cyprus, Cilicia, or northern Syria—and from the Judean Hills. This finding contradicts the often-repeated statements that CBM was mostly produced locally. Furthermore, our study shows that not just Byzantine-period Ashdod but likely the entire southern Levantine coastal strip relied entirely on the importation of roof tiles. The results highlight that multiple Mediterranean workshops participated in producing and exporting roof tiles. Each workshop had both distinctive technological recipes and physical properties depending on the raw materials it employed, usually local soils. This multifaceted provenance of roof tiles within the very same complex also indicates phases of remodeling or extension—the older main complex and the more recent annexes, respectively. To satisfy the demand and need for roof tiles in construction, a large number were imported from overseas. It is likely that due to the lack of local producers on the southern Levantine coast, the import of tons of roof tiles was simply necessary. However, while the import of northeastern Mediterranean roof tiles was probably driven by mercantile logic, the presence of roof tiles from the Judean Hills needs other explanations, such as quality, piety, roof uniformity, or product availability. While the church roof was comprised of various roof tiles with different qualities (along with several other materials, mostly not

preserved), the pigments applied on all roof tile types were identical. They were based on ocher, locally/regionally produced, and applied during the construction process, not before. The location of the mortar remains, always close and parallel to the red paint, supports such a conclusion. Some roof tiles were previously covered in paint before the lines were applied and were probably taken from other roofs.

In sum, this comprehensive investigation sheds light on the intricate dynamics of production, trade, and consumption patterns of roof tiles in Byzantine-period Ashdod-Yam. These interactions reveal a dialogue between local demands, available resources, and economic considerations that shaped the architectural fabric of the period. The discernible preference for certain materials, despite their inherent logistical challenges and costs, highlights the cultural and economic influences driving Late Antiquity building practices and thus offers a tangible reflection of interconnectedness in the eastern Mediterranean world.

Declaration of competing interest

The authors declare that they have no known competing financial interests or personal relationships that could have appeared to influence the work reported in this paper.

Acknowledgments

We thank Ofek Golan of the Center for Nanoscience and Nanotechnology at Tel Aviv University for his valuable SEM technical assistance. We are also grateful to David Ben-Shlomo for his authorization to use laboratory equipment at Ariel University and Barnea Levi Selavan for his useful and profound editing.

Supplementary materials

Supplementary material associated with this article can be found, in the online version, at [doi:10.1016/j.aia.2024.100040](https://doi.org/10.1016/j.aia.2024.100040).

References

- Adan-Bayewitz, D., Perlman, I., 1990. The local trade of Sepphoris in the Roman period. *Israel Explorat. J.* 40 (2/3), 153–172.
- Aharoni, Y., 1962. Excavations at Ramat Rahel, Seasons 1959 and 1960. *Università degli Studi Di Roma. Centro di studi semitici*, Rome.
- Al-Shorman, A.H.B., Al-Muhsen, Z.H., Khalayleh, R.M., Al-Daire, A.A., 2023. The Mineralogical, Chemical and Physical Properties of Ceramic Building Material: Khirbet Edh-Dharib in Southern Jordan (First Century BC – Seventh Century AD). *J. Eastern Mediterranean Archaeol. Heritage Stud.* 11 (4), 390–418.
- Arkin, Y., Braun, M., Starinsky, A., 1965. Type sections of Cretaceous Formations in the Jerusalem – Beit Shemesh Area. Stratigraphic Section 1. Geological Survey of Israel, Jerusalem.
- Arkin, Y., Ecker, A., 2014. Geology of infrastructure and water in Jerusalem. GSI Report No. GSI/08/2014. GSI, Jerusalem.
- Arnold, D., Bourriau, J., 1993. An introduction to ancient Egyptian pottery. Philipp von Zabern, Mainz.
- Arubas, B., Goldfus, H., 1995. The kilnworks of the tenth legion Fretensis. In: Humphrey, J.H. (Ed.), *The Roman and Byzantine Near East – Some recent archaeological research*. University of Michigan Press, Ann Arbor, pp. 95–107.
- Arubas, B., Goldfus, H., 2005. Excavations on the site of the Jerusalem International Convention Center (Binyanē Ha-Umma): a settlement of the Late First to Second Temple Period, The tenth legion's kilnworks, and a Byzantine monastic complex. *J. Roman Archaeol.* 60, 11–16. Supplementary Series.
- Ashkenazi, D., Fantalkin, A., 2019. Archaeometallurgical and archaeological investigation of Hellenistic metal objects from Ashdod-Yam (Israel). *Archaeol. Anthropol. Sci.* 11, 913–935.
- Ashkenazi, D., Shnabel, R., Lichtenberger, A., Tal, O., 2021. Chemical analysis of plaster and pigments retrieved from a decorated house wall at Seleucid Tell Iztabba (Nysa-Scythopolis, Beth She'an, Israel). *Mediterranean Archaeol. Archaeometry* 21 (3), 89–122.
- Bäbler, B., Fantalkin, A., 2023. Azotos paraliōs during the periods of Roman and Byzantine domination: literary sources vs. archaeological evidence. In: Horn, C., Bäbler, B. (Eds.), *Word and space interacting in Palestine in Late Antiquity: Towards a history of pluridimensionality*. Eastern Mediterranean texts and contexts 5, Chesterfield, pp. 89–119.
- Bagatti, D., 1947. I monumenti di Emmaus el-Qubeibeh e dei dintorni. Franciscan Press, Jerusalem.
- Bakler, N., 1982. The geology of Tel Ashdod. In: Dothan, M., Porath, Y. (Eds.), *Ashdod IV. Excavation of Area M. The fortifications of the Lower City*, pp. 65–69. 'Atiqot 15.
- Barkan, D., Yasur-Landau, A., Mommsen, H., Ben-Shlomo, D., Kahanov, Y., 2013. The 'Dor 2006' shipwreck: the ceramic material. *Tel. Aviv.* 40 (1), 117–143.
- Baumgarten, Y.A.Y., 2000. Evidence of a pottery workshop of the byzantine period at the foot of Tel Ashdod ('Ad Halom Site). 'Atiqot 45, 201.
- Ben-Shlomo, D., 2006. Petrographic analysis of Roman-Byzantine roof tiles. 34th International Symposium on Archaeometry, 3–7 May 2004. CSIC, Zaragoza, pp. 413–418.
- Ben-Shlomo, D., 2020. Iron age pottery from the cave of the patriarchs at Hebron. *Israel Explorat. J.* 70 (1), 49–63.
- Ben-Shlomo, D., Mommsen, H., 2018. Pottery production in Jerusalem during the Iron Age: a new compositional profiling. *Geoarchaeology* 33 (3), 349–363.
- Ben-Shlomo, D., Mommsen, H., 2019. New analysis of cylindrical and ovoid jars ('archive jars') from Southern Judea. *Archaeometry* 61 (6), 1264–1279. <https://doi.org/10.1111/arc.12496>.
- Ben-Shlomo, D., Bouzaglou, L., Sterba, J., Mommsen, H., 2022. Production centers of cooking pots in Iron Age Judah. *Archaeometry* 65 (1), 84–104.
- Ben-Tor, Y.K., 1945. Petrographic Investigations of the Upper Albian-Lower Cenomanian near Jerusalem and their contribution to the problem of dolomitization and quartzification. The Hebrew University of Jerusalem. Ph.D. dissertation.
- Bes, P.M., Braekmans, D., forthcoming. Covering the roof. Late Roman roof tiles from Horvat Kur, Galilee (Israel).
- Ben-Tor, Y.K., 1966. The clays of Israel. Guide Book to the excursions of the International Clay Conference. Israel program for scientific translation, Jerusalem.
- Blakely, J.A., Brinkmann, R., Vitaliano, C.J., 1992. Roman mortaria and basins from a sequence at Caesarea: fabrics and sources. In: *Caesarea Papers, Straton's Tower, Herod's harbour, and Roman and Byzantine Caesarea*. *J. Roman Archaeol., Suppl. Series 5*. University of Michigan, Ann Arbor.
- Bourriau, J.D., Smith, L.M.V., Nicholson, P.T., 2000. New Kingdom pottery fabrics: Nile clay and mixed Nile/marl clay fabrics from Memphis and Amarna. *Egypt Exploration Society*, London.
- Bouzaglou, L., forthcoming. The 'Grand Bazaar' of the eastern Mediterranean Sea: ceramic building materials and specialist ceramic vessels at Caesarea Maritima during the Roman and Byzantine Periods. In: *Caesarea Maritima: between past and future conference*.
- Bresson, A., 2016. *The making of the ancient Greek economy: Institutions, markets, and growth in the city-states*. Princeton University Press, Princeton and Oxford (Translated by Steven Rendall).
- Casson, L., 1974. *Travel in the ancient world*. George Allen and Unwin Ltd., London.
- Clermont-Ganneau, C., 1899. *Archaeological researches in Palestine during the years 1893–1894*. Palestine Exploration Fund, London.
- Cohen-Weinberger, A., Goren, Y., 1996. Petrographic analysis of Iron Age 1 Pithoi from Tel Sasa. 'Atiqot 38, 77–83.
- Cohen-Weinberger, A., Szanton, N., Uziel, J., 2017. Ethnofabrics: petrographic analysis as a tool for illuminating cultural interactions and trade relations between Judah and Philistia during the Iron Age II. *Bull. Am. Schools Oriental Res.* 377 (1), 1–20.
- Cohen-Weinberger, A., Rosenthal-Heginbottom, R., 2019. Local and imported Roman ceramics through typological and petrographic analysis. In: Rosenthal-Heginbottom, R. (Ed.), *Jerusalem, Western Wall Plaza Excavations, Vol II, Israel Antiquities Authority Reports 64*. Israel Antiquities Authority, Jerusalem, pp. 249–267.
- Cohen-Weinberger, A., Levi, D., Be'eri, R., 2020. On the raw materials in the ceramic workshops of Jerusalem, before and after 70 CE. *Bull. Am. Schools Oriental Res.* 383 (1), 33–59.
- Cohen-Weinberger, A., Lieberman, T., Szanton, N., 2022. IVL impressions and their implications for the production of ceramic building materials in Aelia Capitolina. *Tel. Aviv.* 49 (1), 98–114.
- Cohen-Weinberger, A., Shimshon-Paran, N., Taxel, I., 2024. Roman-period trade in ceramic building materials on the Levantine Mediterranean coast: evidence from a farmstead site near Ashqelon/Ascalon, Israel. *J. Roman Archaeol.* <https://doi.org/10.1017/S1047759424000102>.
- Coleman, R.G., 1977. *Ophiolites: ancient oceanic lithosphere?* Springer Science and Business Media, Berlin–Heidelberg.
- Dauphin, C., Edelstein, G., 1984. L'Église Byzantine de Nahariya (Israel). Étude Archéologique Kentro Byzantinon Eregon, Thessaloniki.
- Degryse, P., Poblome, J., Donners, K., Deckers, J., Waelkens, M., 2003. Geoarchaeological investigations of the "potters'" quarter at Sagalassos, southwest Turkey. *Geoarchaeology: Int. J.* 18 (2), 255–281.
- Dilek, Y., Eddy, C.A., 1992. The Troodos (Cyprus) and Kizildag (S. Turkey) ophiolites as structural models for slow-spreading ridge segments. *J. Geol.* 100 (3), 305–322.
- Dilek, Y., Furnes, H., 2014. Ophiolites and their origins. *Elements* 10 (2), 93–100.
- Di Segni, L., Bouzaglou, L., Fantalkin, A., 2022. A recently discovered church at Ashdod-Yam (Azotos Paraliōs) in light of its Greek Inscriptions. *Liber Annuus* 72, 399–447. <https://doi.org/10.1484/J.LA.5.134545>.
- Domingo, I., Chieli, A., 2021. Characterizing the pigments and paints of prehistoric artists. *Archaeol. Anthropol. Sci.* 13, 1–20.
- Ebeling, P., Barford, G.H., 2022. An archaeo-scientific analysis of building ceramics from the Northwest Quarter. In: Lichtenberger, A., Raja, R. (Eds.), *Architectural elements, wall paintings, and mosaics: Final Publications from the Danish-German Jerash Northwest Quarter Project 4.1*. Brepols, Turnhout, pp. 171–189.
- Edwards, D.R., 2009. Walking the Roman landscape in Lower Galilee: Sepphoris, Jotapatra, and Khirbet Qana. In: Rodgers, Z., Daly-Denton, M., Fitzpatrick-McKinley, A. (Eds.), *A wandering Galilee: essays in honour of Seán Freyne*. Brill, Leiden, Boston, pp. 219–236.
- Eiland, M.L., Williams, Q., 2001. Investigation of Islamic ceramics from Tell Tuneinir using X-ray diffraction. *Geoarchaeology: Int. J.* 16, 875–903.
- Eramo, G., 2020. Ceramic technology: how to recognize clay processing. *Archaeol. Anthropol. Sci.* 12 (8), 164 paper no.
- Fantalkin, A., 2014. Ashdod-Yam on the Israeli Mediterranean coast. A first season of excavations. *Skyllis* 14, 45–57.
- Fantalkin, A., 2018. Neo-assyrian involvement in the southern coastal plain of Israel: old concepts and new interpretations. In: Zelig Aster, S., Faust, A. (Eds.), *The southern Levant under Assyrian domination*. Eisenbrauns, Winona Lake, pp. 162–185.
- Fantalkin, A., Johananoff, M., Krispin, S., 2016. Persian-period Philistia coins from Ashdod-Yam. *Israel Numismatic J.* 11, 23–28.
- Fantalkin, A., Itkin, E., Chesnut, O., Mazis, M., Lorenzon, M., Bouzaglou, L., Eshel, T., Sharvit, J., 2024a. Iron age remains from Ashdod-Yam: An interim report (2013–2019). *J. East. Mediterr. Archaeol. Herit. Stud.* 12/3, 250–297.
- Fantalkin, A., Mazis, M., Schauer, Y., Ariel, D.T., Krispin, S., Tsuf, O., Eshel, T., Itkin, E., 2024b. Hellenistic Ashdod-Yam in light of recent archaeological investigations. *Tel Aviv.* 51 (2), 238–278.
- Fitzgerald, G.M., 1931. *Beth-Shan Excavations 1921–1923: The Arab and Byzantine Levels*. Publications of the Palestine section of the museum of the University of Pennsylvania, 3. University Press, Philadelphia.
- Ganor, S., 2017. *Horbat Ashdod-Yam, HA-ESI 129*: http://www.hadashot-esi.org.il/report_detail_eng.aspx?id=25173&mag_id=125.
- Garzanti, E., Ando, S., Scutella, M., 2000. Actualistic ophiolite provenance: the Cyprus case. *J. Geol.* 108 (2), 199–218.
- Geva, H., 2003. Miscellaneous finds. In: Geva, H. (Ed.), *Jewish Quarter excavations in the Old City of Jerusalem, conducted by Nahman Avigad, 1969–1982, Volume 2: The finds from Area A, W and X-2*. Final report. Institute of Archaeology, Hebrew University of Jerusalem, Jerusalem.

- Glass, J., 1980. Petrological analysis of a Type A tegula. In: Briend, J., Humbert, J.-B. (Eds.), *Tell Keisan (1971–1976): Une cité Phénicienne en Galilée, orbis biblicus et orientalis series archaeologica*, 1. Gabalda, Paris, p. 87.
- Goren, Y., 1995. Shrines and ceramics in Chalcolithic Israel: the view through the petrographic microscope. *Archaeometry*. 37 (2), 287–305.
- Goren, Y., 1996a. The southern Levant during the Early Bronze Age IV: the petrographic perspective. *Bull. Am. Schools Oriental Res.* 303 (1), 33–72.
- Goren, Y., 1996b. Petrographic study of the pottery assemblage. In: Gopher, A. (Ed.), *The Nahal Qanah cave: earliest gold in the southern Levant*. Institute of Archaeology, Tel Aviv University, Tel Aviv, pp. 147–154.
- Goren, Y., Finkelstein, I., Na'aman, N., 2004. Inscribed in clay. Provenance study of the Amarna letters and other ancient Near Eastern texts. Tel Aviv University, Tel Aviv.
- Green, J., 1971. An underwater archaeological survey of Cape Andreas, Cyprus 1969–1970: a preliminary report. In: Blackman, D.J. (Ed.), *Maritime Archaeology: Proceedings of the 23 Symposium 1971 of the Colston Research Society held in the University of Bristol*, 4–8 April. Butterworth, London, pp. 141–179.
- Green, J., 2019. Legacy data in 3D: the cape andreas survey (1969–1970) and *Santo António de Tanná* expeditions (1978–1979). In: McCarthy, J.K., Benjamin, J., Winton, T., van Duivenvoorde, W. (Eds.), *3D recording and interpretation for Maritime Archaeology*. Springer, Cham, pp. 29–43.
- Giumlia-Mair, A.R., Sedov, V.V., Vdovichenko, M.V., Riccardi, M.P., 2022. On blue and green pigments from the St. George Cathedral of Veliky Novgorod. *Adv. Archaeomater.* 3 (2), 109–119. <https://doi.org/10.1016/j.aia.2023.06.001>.
- Hampe, R., Winter, A., 1965. Bei Töpfern und Zieglern in Süditalien, Sizilien und Griechenland. Römisch-Germanisches Zentralmuseum, Mainz.
- Holmqvist-Sipilä, E., 2019. Ceramics in transition: production and exchange of Late Byzantine – Early Islamic pottery in southern Transjordan and the Negev. *Archaeopress*, Oxford.
- Ion, R.M., Barbu, M.G., Gonciar, A., Vasilevici, G., Gheboianu, A.I., Slamnoiu-Teodorescu, S., David, M.E., Iancu, L., Grigorescu, R.M., 2022. A multi-analytical investigation of Roman frescoes from Rapoltu Mare (Romania). *Coatings* 12 (4), 530. <https://doi.org/10.3390/coatings12040530> paper no.
- Jacobs, A., Borgers, B., 2015. Assessing ceramic variability of plain ware products. In: Jacobs, A., Nys, K. (Eds.), *Cypriot material culture and heritage Studies: From picrolite carving to proskynetaria*, Proceedings of the eighth annual postgraduate Cypriot archaeology conference held in memory of Paul Åström, Brussels (27 to 29th November 2008). Uitgeverij VUB, Brussels, pp. 93–113.
- Kaplan, J., 1969. The stronghold of Yamani at Ashdod-Yam. *Israel Exploration J.* 19, 137–149.
- Kingsley, S.A., 2003. The Dor D shipwreck and Holy Land wine trade. *Int. J. Nautical Archaeol.* 32, 85–90.
- Kretz, R., 1983. Symbols of rock-forming minerals. *Am. Mineral.* 68, 277–279.
- Landgraf, J., 1980. Roof tiles. In: Briend, J., Humbert, J.B. (Eds.), *Tell Keisan (1971–1976): Une cité Phénicienne en galilée. Orbis biblicus et orientalis series archaeologica*, 1. Gabalda, Paris, pp. 83–87.
- Lombardi, G., 1957. Bolli Bizantino-Arabi al “Dominus Flevit. *Liber Annuus* 7, 165–190.
- Lorenzon, M., Cutillas-Victoria, B., Itkin, E., Fantalkin, A., 2023. Masters of mudbrick: geoarchaeological analysis of Iron Age earthen public buildings at Ashdod-Yam (Israel). *Geoarchaeology*. 35–63. <https://doi.org/10.1002/gea.21977>.
- Lorenzon, M., Posada, L.R., Gkouma, M., Bouzaglou, L., Ebeling, P., Fantalkin, A., forthcoming. From earth to eternity: investigating the use of clay and bitumen in the byzantine church construction at Ashdod-Yam.
- Magen, Y., 2015. *Monastery of Martyrius. Christians and Christianity*, 5. Judea and Samaria Publications, 17. Israel Antiquities Authority, Jerusalem.
- Magen, Y., Baruch, Y., 2012. ‘Khirbet Abu Rish’, Christians and Christianity, 4. Churches and monasteries in Judea. Judea and Samaria Publications, 16. Israel Antiquities Authority, Jerusalem.
- Magen, Y., Har-Even, B., Sharukh, I., 2012. Roman tower and a Byzantine monastery at Khirbet el-Qasr, Christians and Christianity, 4. Churches and monasteries in Judea. Judea and Samaria Publications, 16. Israel Antiquities Authority, Jerusalem.
- Makarona, C., Mattielli, N., Laha, P., Terry, H., Nys, K., Claeys, P., 2016. Leave no mudstone unturned: geochemical proxies for provenancing mudstone temper sources in South-Western Cyprus. *J. Archaeol. Sci.: Reports* 7, 458–464.
- Manning, S.W., Sewell, D.A., Herscher, E., 2002. Late Cypriot IA maritime trade in action: underwater survey at Maroni Tsaroukkas and the contemporary east Mediterranean trading system. *Ann. Br. School Athens* 97, 97–162.
- Mazar, E., 2007. The Temple Mount excavations in Jerusalem 1968-1978 Directed by Benjamin Mazar: Final reports 3: The Byzantine period. Qadem 46. Hebrew University of Jerusalem, Jerusalem.
- Mikhailov, I., Ponikarov, V., 1986. Geological Map of Syria 1: 1,000,000. Syrian Arab Republic, Ministry of Industry. Department of Geological and Mineral Research, Damascus.
- Mills, P., 2013. The ancient Mediterranean trade in ceramic building materials: A case study in Carthage and Beirut. *Archaeopress*, Oxford.
- Mills, P., 2015a. The potential of ceramic building materials in understanding late antique archaeology. In: Lavan, L., Mulryan, M. (Eds.), *Field methods and post-excavation techniques in Late Antique archaeology*. Leiden and Boston, Brill, pp. 573–594.
- Mills, P., 2015b. The social life of tile in the Roman world. In: DeLaine, J., Camporeale, S., Pizzo, A. (Eds.), *Arqueología de la construcción 5: Manmade material, engineering and infrastructure. Anejos de archivo Español de arqueología*, 77. Instituto Arqueología Mérida, Madrid, pp. 87–97.
- Miyashiro, A., 1975. Classification, characteristics, and origin of ophiolites. *J. Geol.* 83 (2), 249–281.
- Mommsen, H., Ben-Shlomo, D., 2020. Compositional analysis of cylindrical and ovoid jars (“archive jars”) and other vessels from Hebron, Jericho, and Masada. *Judea Samaria Stud.* 29 (1), 49–90. <https://doi.org/10.26351/JSRS/29-1/7>.
- Mommsen, H., Sjöberg, B.L., 2007. The importance of the ‘best relative fit factor’ when evaluating elemental concentration data of pottery demonstrated with mycenaean sherds from Sinda, Cyprus. *Archaeometry*. 49 (2), 359–371. <https://doi.org/10.1111/j.1475-4754.2007.00306.x>.
- Mommsen, H., Beier, T., Hein, A., Ittameier, D., Podzuweit, C., 1995. Ceramic production and distribution in bronze age settlements in greece - status report of neutron activation analysis results. *Monogr. Mater. Soc.* 2, 513–520.
- Moore, E.M., 1982. Origin and emplacement of ophiolites. *Rev. Geophys.* 20 (4), 735–760.
- Müller, N.S., 2017. Mechanical and thermal properties. In: Hunt, A.M.W. (Ed.), *The Oxford handbook of archaeological ceramic analysis*. Oxford University Press, Oxford, pp. 603–624. Press.
- Munteanu, C., Vochițu, A., 2010. Roof tiles from the ancient Greek shipwreck ‘Mangalia B’, Black Sea coast, Romania. *Int. J. Naut. Archaeol.* 39 (2), 407–412.
- Nicolas, A., 2012. Structures of ophiolites and dynamics of oceanic lithosphere (vol. 4). Springer Science and Business Media, Berlin–Heidelberg.
- Nicolas, A., Boudier, F., 2003. Where ophiolites come from and what they tell us. *Geol. Soc. Am. Special Papers* 373, 137–152.
- Nodarou, E., 2017. An analytical study of the pithoi from Alassa. In: Hadjisavvas, S. (Ed.), *Alassa. Excavations at the Late Bronze age sites of Pano Mantilaris and Paliotaverna 1984-2000*. Cyprus Department of Antiquities, Lefkosia, pp. 629–641.
- Parrot, J.F., 1977. Assemblage ophiolitique du Baër-Bassit et termes effusifs du volcanosédimentaire: Pétrologie d’un fragment de la croûte océanique Téthysienne charriée sur la plate-forme Syrienne. O. R. S. T. O. M., Paris.
- Peilstöcker, M., 2009. Tel ‘Afar: a Byzantine site south of Caesarea. *‘Atiqot* 61, 95–118.
- Pele, O., 2003. Roof tiles of the Byzantine period from Area XV. In: Mazar, E. (Ed.), *The Temple Mount excavations in Jerusalem 1968-1978 Directed by Benjamin Mazar: Final reports 2: The Byzantine and Early Islamic periods*. Qadem 43. Hebrew University of Jerusalem, Jerusalem, pp. 133–134.
- Peleg, M., Reich, R., 1992. Excavations of a segment of the Byzantine city wall of Caesarea Maritima. *‘Atiqot* 21, 137–170.
- Peloschek, L., 2015. Cultural transfers in Aswan (Upper Egypt): Petrographic evidence for ceramic production and exchange from the Ptolemaic to the Late Antique period. University Wien. PhD dissertation.
- Pertman, I., Frank, A., 1969. Pottery analysis by neutron activation. *Archaeometry*. 11, 21–52.
- Pipano, S., 1990. The history of Ashdod-Yam in the Byzantine period. In: Ra’anana, B. (Ed.), *Ashdod geography, history, nature and short hikes*. Society for the Protection of Nature, Ashdod, pp. 143–146 (Hebrew).
- Quinn, P.S., 2013. Ceramic petrography: the interpretation of archaeological pottery and related artefacts in thin section. In: Quinn, P.S. (Ed.), *Ceramic Petrography*. Archaeopress, Oxford.
- Quinn, P.S., 2022. Thin section petrography, geochemistry and scanning electron microscopy of archaeological ceramics. *Archaeopress*, Oxford.
- Raphael, S.K., 2014. *Azdud (Ashdod-Yam): An Early Islamic fortress on the Mediterranean coast*. Archaeopress, Oxford.
- Rapuan, Y., 2016. The pottery from the church of Bishop Johannes at Horvath Barqa, Gan Yavne. *‘Atiqot* 84, 115–118.
- Rautman, M.L., Basil, G., Neff, H., Glascock, M.D., 1993. Neutron Activation Analysis of Late Roman ceramics from Kalavassos – Kopetra and the environs of the Vasilikos Valley. Reports of the Department of Antiquities of Cyprus, pp. 233–265.
- Rautman, M.L., Neff, H., Gomez, B., Vaughan, S., Glascock, M.D., 1999. Amphoras and roof tiles from Late Roman Cyprus: a compositional study of calcareous ceramics from Kalavassos-Kopetra. *J. Roman Archaeol.* 12, 377–391.
- Reeves, B.M., Harvey, G.A., 2016. A typological assessment of the Nabataean, Roman and Byzantine ceramic building materials at Al-Humayma and Wadi Ramm. *Stud. History Archaeol. Jordan* 12, 443–475.
- Reich, R., Shukron, E., 2006. Excavations in the Mamillah Area, Jerusalem: the Medieval fortifications. *‘Atiqot* 54, 125–152.
- Rice, P.M., 2015. *Pottery analysis: A sourcebook*, 2nd ed. University of Chicago Press, Chicago/London.
- Saller, S., 1957. *Excavations at Bethany (1949–1953)*. Franciscan Press, Jerusalem.
- Saller, S., 1946. *Discoveries at St. John’s, ‘Ein Karim, 1941–1942*. Franciscan Press, Jerusalem.
- Seligman, J., Gagoshidze, I., 2015. A Georgian monastery from the Byzantine period at Khirbat Umm Leisun, Jerusalem. *‘Atiqot* 83, 145–179.
- Şenel, M., 2002. Geological Map of Turkey 1:500,000: Hatay. General directorate of mineral research and exploration. Ankara (Turkish and English).
- Shapiro, A., 1997. Petrographic analysis of Roman clay sarcophagi from Northwestern Israel and Cyprus. *‘Atiqot* 33, 1–5.
- Shapiro, A., 2017. Petrographic examination of tiles, bricks and mortaria from Legio. *‘Atiqot* 89, 41–47.
- Sion, O., 2016. The church of Bishop Johannes at Horbat Barqa, Gan Yavne. *‘Atiqot* 84, 79–88 (Hebrew, with an English abstract on p. 128).
- Sterba, H., 2015. Neutron Activation Analysis of samples from pottery, kiln and soil in Nakadake Sanroku and related sites in south Japan. In: Nakamura, N., Shinoto, M. (Eds.), *Studies on the Nakadake Sanroku kiln site cluster*. Research Center for Archaeology, Kagoshima, pp. 67–71.
- Sterba, J.H., 2018. A workflow for Neutron Activation Analysis of archaeological ceramics at the Atominstitut in Vienna, Austria. *J. Radioanal. Nucl. Chem.* 316 (2), 753–759.

- Sultana, M.S., Ahmed, A.N., Zaman, M.N., Rahman, M.A., Biswas, P.K., Nandy, P.K., 2015. Utilization of hard rock dust with red clay to produce roof tiles. *J. Asian Ceramic Soc.* 3 (1), 22–26.
- Tekeli, O., Erendil, M., 1986. Geology and petrology of the Kizilıdađ ophiolite (Hatay). *Bull. Mineral Res. Explor.* 107, 24–40.
- Tepper, Y., Jonathan David, J., Adams, M.J., 2016. The Roman Vith legion Ferrata at Legio (el-Lajjun), Israel: preliminary report of the 2013 excavation. *STRATA, Bull. Anglo-Israel Archaeol. Soc.* 34, 91–123.
- Tsafiri, Y., Di Segni, L., Green, J., 1994. *Tabula Imperii Romani – Judaea-Palaestina: Eretz Israel in the Hellenistic, Roman and Byzantine periods.* The Israel Academy for Sciences and Humanities, Jerusalem.
- Tsafiri, Y., Hirschfeld, Y., Drory, J., 1979. The church and mosaics at Horvat Berachot, Israel. *Dumbarton Oaks Papers* 33, 291–326.
- Vaughan, S.J., 1987. A fabric analysis of Late Cypriot base ring ware: studies in ceramic technology, petrology, Geochemistry and Mineralogy. University College London. Doctoral dissertation.
- Vriezen, K.J.H., 1994. *Die Ausgrabungen unter der Erlöserkirche im Muristan, Jerusalem (1970-1974).* Harrassowitz, Wiesbaden.
- Vriezen, K.J.H., 1995. A preliminary study of the Byzantine roof Tiles (tegulae and imbreces) from Areas I and III in Umm Qeis (Jordan), 13. *Newsletter of the Department of Pottery Technology (Leiden University)*, pp. 26–40.
- Vriezen, K.J.H., Mulder, N.F., 1997. Umm Qays: the Byzantine buildings on the terrace. The building materials of stone and ceramics. *Stud. History Archaeol. Jordan* 4, 323–330.
- Whitbread, I.K., 1995. *Greek transport amphorae: a petrological and archaeological study.* The British School at Athens, Athens.
- Whitechurch, H., Juteau, T., Montigny, R., 1984. Role of eastern Mediterranean ophiolites (Turkey, Syria, Cyprus) in the history of the Neo-Tethys. In: Dixon, J.E., Robertson, A.H.F. (Eds.), *Geological Society. Special Publications*, London, pp. 301–317, 17.
- Williams, D., 2002. A note on the petrology of pottery and tile from the Dor D wreck. In: Kingsley, S.A. (Ed.), *A sixth-century AD shipwreck off the Carmel coast, Israel. Dor D and Holy Land wine trade.* Archaeopress, Oxford, pp. 111–112.
- Zelinger, Y., Barbé, H., 2017. A Byzantine monastery in Nahal Qidron, Jerusalem. *Atiqot* 89, 49–82.
- Xenophontos, C., Pilides, D., Malpas, J.G., 2000. Petrographic analysis of Late Bronze Age Pithoi from Cyprus. In: Despina, P. (Ed.), *Pithoi of the Late Bronze Age in Cyprus: Types from the major sites of the period.* Department of Antiquities of Cyprus, Nicosia, pp. 165–180.

Further reading

- Ebeling P., Bouzoglou, L. and Fantalkin, A. forthcoming. Investigating the 'chaîne opératoire' of Byzantine roof tile production: a case study from Ashdod-Yam's Church.